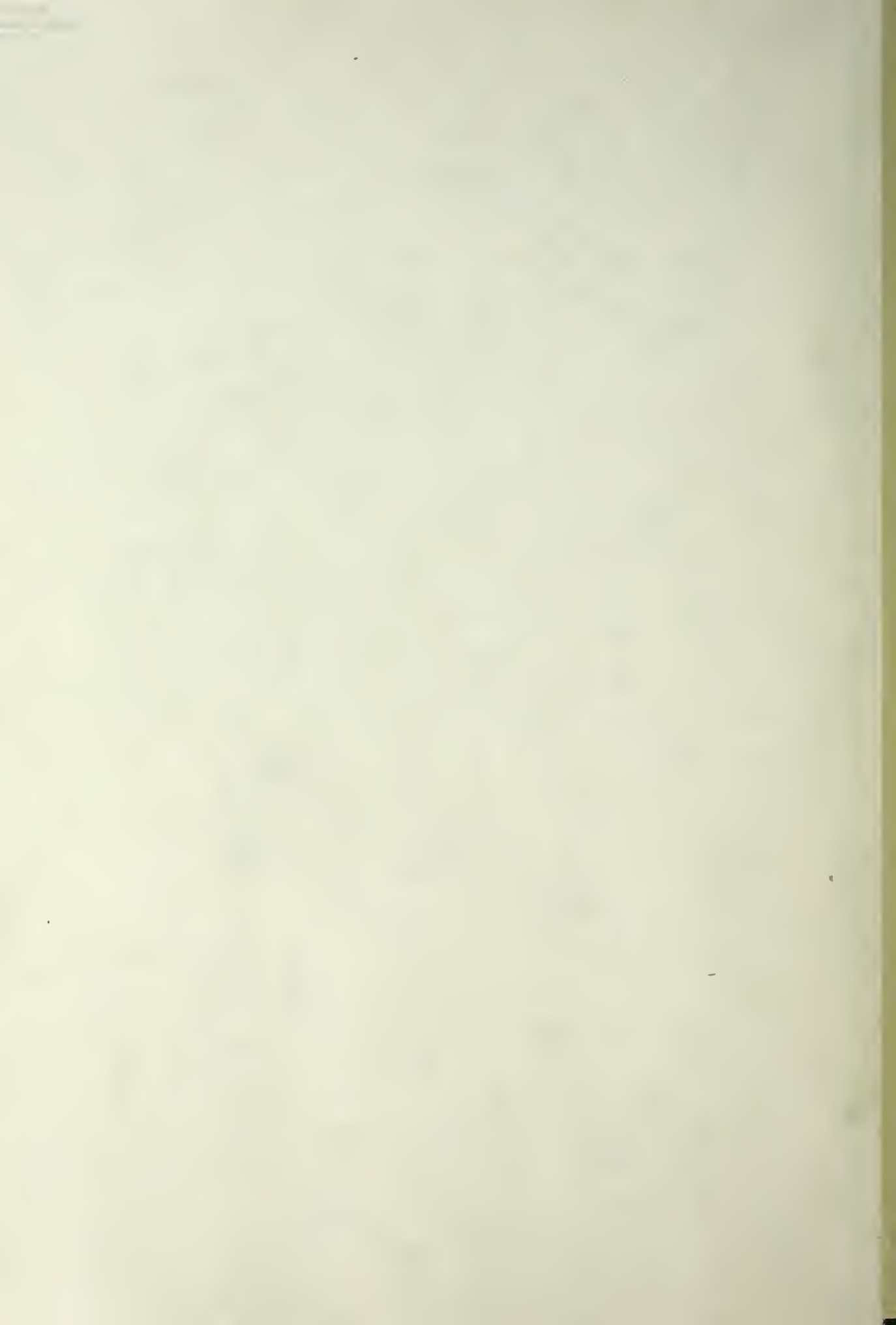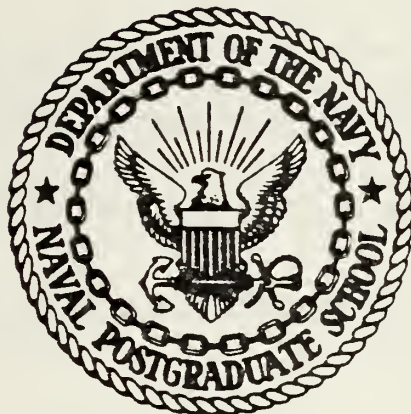# COMPUTER PROGRAM FOR THE KINETICS AND POPULATIONS IN A XENON FLUORIDE LASER

Lonnie William Cole

NAVAL POSTGRADUATE SCHOOL
Monterey, California

THESIS

COMPUTER PROGRAM FOR THE KINETICS AND

POPULATIONS IN A XENON FLUORIDE LASER

by

Lonnie William Cole

December 1979

Thesis Advisor: A. E. Fuhs

NAVAL POSTGRADUATE SCHOOL
Monterey, California

Rear Admiral T.F. Dedman   Jack R. Borsting
Superintendent   Provost

REPORT DOCUMENTATION PAGE

1. REPORT NUMBER	2. GOVT ACCESSION NO.	3. RECIPIENT'S CATALOG NUMBER
NPS-69-79-013		

4. TITLE (and Subtitle)	5. TYPE OF REPORT & PERIOD COVERED
Computer Program for the Kinetics and Populations in a Xenon Fluoride Laser	Master's Thesis; December 1979
	6. PERFORMING ORG. REPORT NUMBER NPS 69-79-013

7. AUTHOR(s)	8. CONTRACT OR GRANT NUMBER(s)
Lonnie William Cole	DARPA Order No. 3747

9. PERFORMING ORGANIZATION NAME AND ADDRESS	10. PROGRAM ELEMENT, PROJECT, TASK AREA & WORK UNIT NUMBERS
Naval Postgraduate School Monterey, California 93940	Program Element: 62301E

11. CONTROLLING OFFICE NAME AND ADDRESS	12. REPORT DATE
Defense Advanced Research Projects Agency 1400 Wilson Blvd Arlington, Virginia 22209	December 1979
	13. NUMBER OF PAGES 85

14. MONITORING AGENCY NAME & ADDRESS(If different from Controlling Office)	15. SECURITY CLASS. (of this report)
Office of Naval Research Code 421 800 Quincy Avenue Arlington, Virginia 22217	Unclassified
	15a. DECLASSIFICATION/DOWNGRADING SCHEDULE

16. DISTRIBUTION STATEMENT (of this Report)

Approved for public release; distribution unlimited.

17. DISTRIBUTION STATEMENT (of the abstract entered in Block 20, If different from Report)

18. SUPPLEMENTARY NOTES

19. KEY WORDS (Continue on reverse side if necessary and identify by block number)

Excimer laser, laser kinetics, population distributions

20. ABSTRACT (Continue on reverse side if necessary and identify by block number)

To highlight in a qualitative manner the kinetics of an excimer laser, a simple computer model for calculating the species populations in a KrF laser cavity is developed; subsequently a computer program originally developed at the Naval Research Laboratory (NRL) is modified to calculate the population of the different electronic configurations of excited neon present in a XeF laser. When modified, the NRL

program accounts for 185 reactions and requires 9.5 minutes of CPU time using the IBM 360/67. The populations obtained are applied to the calculation of the index of refraction in the laser cavity. The phase shift is determined per unit length for two laser wavelengths; one laser wavelength is non-resonance with neon and the other is at resonance. Neon is the dominant specie relative to concentration and within the population distribution the neon ground state dominates by a factor of a million. The calculations show that the ground state neon determines the index of refraction; an exception occurs if the laser wavelength is near resonance to any of the transitions in the $3s \rightarrow 4p$ array. As long as the laser is operated away from the $3s \rightarrow 4p$ resonant wavelengths, the phase shift will be negligibly small resulting in satisfactory beam quality; the preceding statement is valid only for the influence of neon.

Computer Program for the Kinetics and

Populations in a Xenon Fluoride Laser

by

Lonnie William Cole
Lieutenant, United States Navy
B. S., United States Naval Academy, 1973

Submitted in partial fulfillment of the
requirements for the degree of

MASTER OF SCIENCE IN ENGINEERING SCIENCE

from the
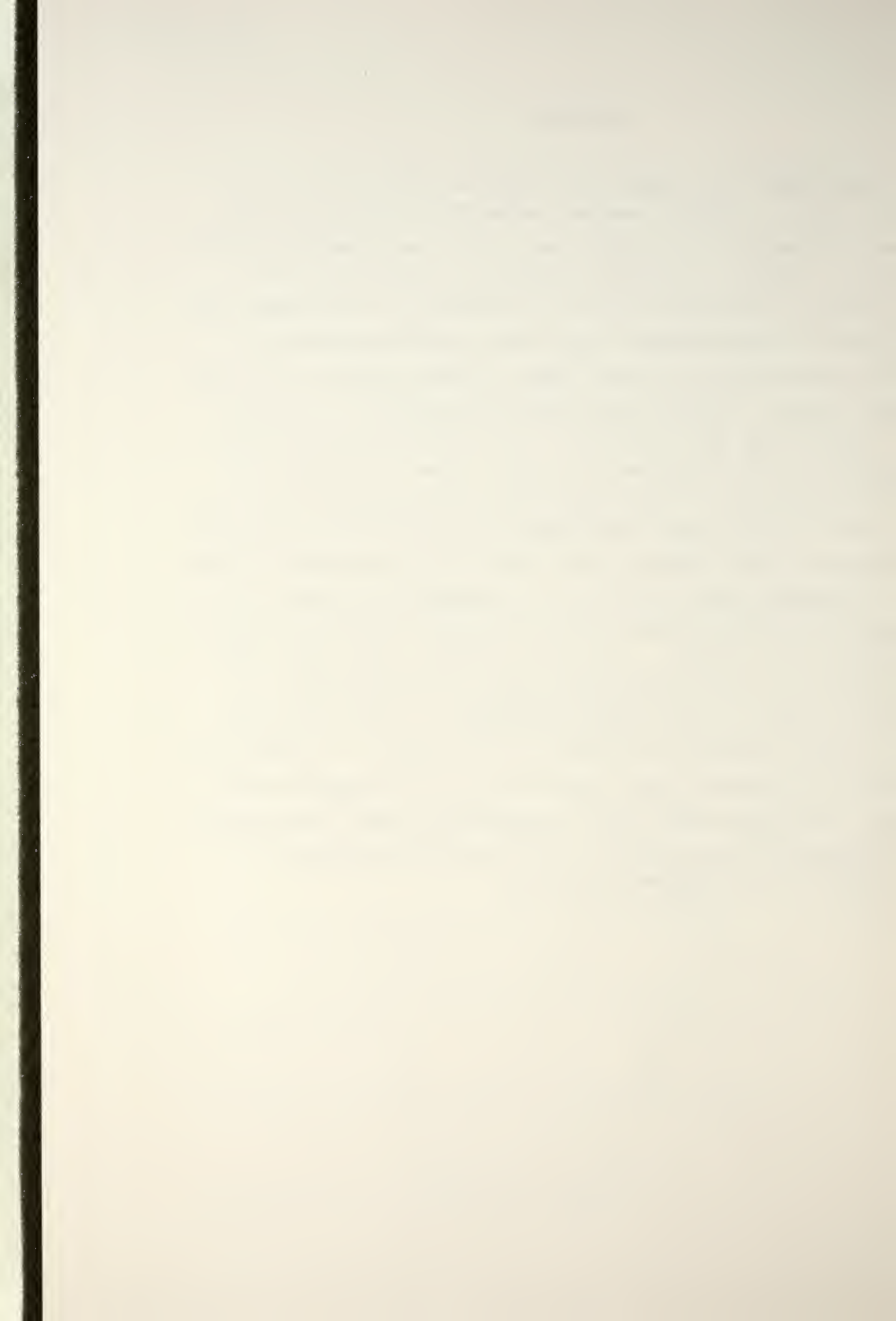NAVAL POSTGRADUATE SCHOOL
December 1979

ABSTRACT

To highlight in a qualitative manner the kinetics of an
excimer laser, a simple computer model for calculating the
species populations in a KrF laser cavity is developed; sub-
sequently a computer program originally developed at the
Naval Research Laboratory (NRL) is modified to calculate the
population of the different electronic configurations of
excited neon present in a XeF laser. When modified, the NRL
program accounts for 185 reactions and requires 9.5 minutes
of CPU time using the IBM 360/67. The populations obtained
are applied to the calculation of the index of refraction
in the laser cavity. The phase shift is determined per unit
length for the two laser wavelengths; one laser wavelength is
non-resonance with neon and the other is at resonance. Neon
is the dominant specie relative to concentration and within
the population distribution the neon ground state dominates
by a factor of a million. The calculations show that the
ground state neon determines the index of refraction; an
exception occurs if the laser wavelength is near resonance
to any of the transitions in the $3s \rightarrow 4p$ array. As long as
the laser is operated away from the $3s \rightarrow 4p$ resonant wave-
lengths, the phase shift will be negligibly small resulting
in satisfactory beam quality; the preceding statement is
valid only for the influence of neon.

TABLE OF CONTENTS

LIST OF TABLES

LIST OF FIGURES

ACKNOWLEDGMENTS

The author would like to acknowledge the support of the Defense Advanced Research Projects Agency (DARPA), for providing the necessary funding for this research project.

First, I would like to express my deepest thanks to my thesis advisor, Dr. Allen E. Fuhs, Distinguished Professor of Mechanical and Aeronautical Engineering, whose untiring assistance made the completion of this thesis possible. If there exists an award for "Professorship" above and beyond the call of duty; Dr. Fuhs most assuredly deserves one.

Second, I am indebted to Dr. Louis J. Palumbo for the assistance rendered in modifying the computer program he provided from NRL. I am also grateful to Jane Foust and Richard Donat of the Naval Postgraduate School Computer Center, who assisted in computer program modification.

Lastly, I would like to thank all the members of the Mechanical Engineering staff who assisted in many important ways on this thesis. Also, the unselfish service of the Educational Media Department Graphics and Photo Lab personnel is sincerely appreciated.

This thesis is dedicated to my wife whose support and devotion throughout my graduate studies has raised me to this new plateau.

8

I. INTRODUCTION

The rare-gas monohalides, such as XeF, are simple diatomic molecules whose properties and emission spectra were essentially unknown as recently as five years ago. Now they are the active media for gas lasers that could provide overall electrical efficiency as high as 10 per cent in various wavelengths, as depicted in Table I.

Table I. Rare-gas Halide Laser Emission Wavelengths

Peak wavelengths of most intense band (nm)

	Ne	Ar	Kr	Xe
F	107[a]	193	248	351,353
Cl	b	170	222	308
Br	b	166[a,b]	206[a]	282
I	b	b	185[a,b]	252[a]

[a]Has not demonstrated laser oscillation.

[b]Predissociates, hence emission is weak or unobservable.

The overall efficiency as explained by J. J. Ewing and C. A. Brau [1] is

> ...a product of a quantum efficiency, an upper laser level production efficiency, an extraction efficiency, an efficiency for producing the initial excited states by the pump, and an energy coupling efficiency which describes the efficiency with which energy gets from a wall socket into the gas medium. The extraction efficiency is comprised of both spectroscopic and kinetic extraction efficiencies

depending on the ratio of net gain to loss and the ratio of rates of stimulated emission of upper laser levels to the quenching and spontaneous loss of upper levels. Certain rare gas halide lasers have potential for high power and high efficiency because they have high efficiency in each of the above mentioned elements. Depending on the application requirements, one may accept a lower efficiency of one of these elements if the compromise allows for some simplification of the laser. Typically this trade off usually involves coupling and excited state production efficiencies.

Rare-gas monohalides belong to a larger class of molecules broadly known as excimers. An excimer is an atomic or molecular aggregate, composed of two atoms or molecules, that is bound in its excited state but is unstable or slightly bound in the ground state.

The term "excimer" is standard chemical nomenclature for dimers which are bound in the excited state and free in the lower state. In standard nomenclature dimer means two of the same thing. Thus, Xe_2^*, Ar_2^*, etc. are excimers. Species that are heteronuclear such as LiXe* or KrF* also can have bound excited states and dissociative lower states. The accepted chemical nomenclature for such species is "exciplex" short for excited complex. Unfortunately, the laser community has not uniformly utilized good scientific English and typically calls all species with dissociative lower states, and even some like XeF with slightly bound lower states, "excimers".

The excited state of the excimer species can radiate in a broad band that is red shifted from the wavelength of the parent atomic excitation. The size of the bandshift

depends on the depth of the excited state well (typically
1-5eV) and on the repulsion of the lower state at the energy
minimum of the excimer. In Figure 1 are schematic potential
energy curves for an excimer.

INTERNUCLEAR SEPARATION
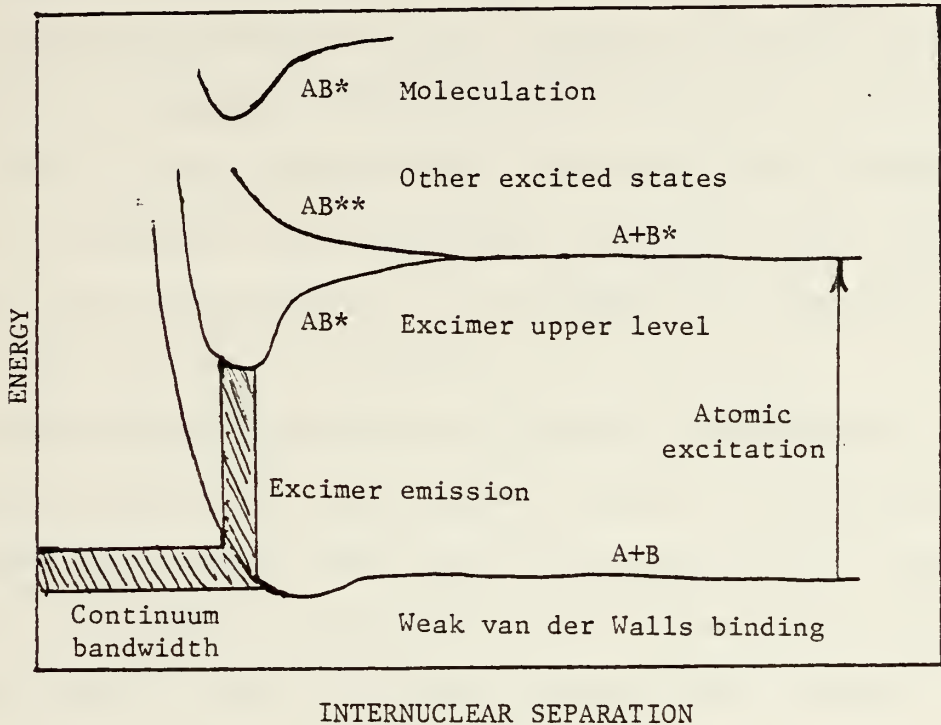
Figure 1. Potential Energy of Excimers (Reproduced from
Ewing [2].

Excimer emission spectra are useful for lasers because
the lower level rapidly dissociates. Since the dissociation
time, about 10^{-12} second, is much less than upper level
radiative lifetimes, 10^{-9} to 10^{-6} second, population inver-
sions can be readily produced and maintained.

The excimer laser or exciplex laser offers features
which are essential for military applications [2-4]. These
features are as follows: first, the potential for high
efficiency; second, scalability to large volume and high
power; and, third, transmission through the atmosphere

using either directly-generated photons or frequency-converted photons [5]. As a result of the attractive characteristics, considerable effort has been and is being directed toward identification of key technical issues and establishment of feasible solutions to the problems identified [6-11]. In addition to research directed toward the laser device itself, work is also being funded on related and relevant aspects, including e-beam technology, UV optics, and time dependent laser aerodynamics. For example, see Bennett, et al. [12] for work on UV optics.

Systems studies have been conducted by Rocketdyne. Among the various aspects of large excimer lasers considered in the Rocketdyne reports was beam quality as influenced by non-uniformity of index of refraction. The adverse impact of poor beam quality upon the overall system was stressed.

For military applications the optimum pulse duration should be a few microseconds [13-15]. The pulse duration for some military applications is in contrast to the desired pulse duration of a few nacoseconds for inertial confinement to achieve thermonuclear fusion [1]. Even if a pulse duration of 10 microseconds is used, the motion of the waves, e.g., cathode shock wave and anode wave, in the gas will be very small, i.e., of the order of

$$\ell = a \tau = (300 \text{ m/sec}) (10^{-5} \text{ sec}) = 3 \text{ mm} \quad (1)$$

where a is the acoustic wave speed and τ is the pulse duration. However, this fact does not suggest that a pulsed

excimer laser will be free of inhomogeneity problems; exten-
sive experience with pulsed electrical lasers operating in
the IR indicates that beam quality may be a problem. To
achieve high average power, a large pulse repetition fre-
quency, PRF, must be used which requires a flowing laser.
The higher the PRF, the faster the gas flow is.

Gas flow in a high power, high PRF, excimer laser will
probably be subsonic. In subsonic flow [16-18], disturbances
can propagate upstream. Even if the upstream base flow is
perfect, the gas moving out of the cavity after a pulse can
cause $\Delta n/n$ within the cavity; n is index of refraction, and
Δn is spatial variation of index of refraction. A large
flush factor eases the problem of a nonuniform base flow;
however, high efficiency demands a low flush factor.

Nonuniformity of the lasing medium may have adverse
effects distinct from the deterioration of beam quality.
The work of Nerheim and Chen [19] at JPL indicates different
levels of performance depending on homogeneity of the gas.
Pulses into a homogeneous medium resulted in one level of
power output; pulses into an inhomogeneous medium yielded
another level (lower naturally) of performance. Details of
the physics involved in this observation were not unraveled.
The work by Nerheim and Chen was with an atomic copper laser.
Consequently the results are not directly transferable to
rare gas-halide lasers.

Despite the many unsolved problems regarding excimer
lasers, its use as a potential weapon constitutes a

revolution greater than the leap from naval guns to guided missiles. Some of the conceivable missions for the excimer laser are ballistic missile defense (both ground-based silo defense and space-based destruction of ICBMs in the boost phase), space-based antisatellite defense, and antiship missile defense (ASMD) [20]. The latter has the most promise of relatively near-term development. Also, the radiation from certain excimer lasers has good propagation in sea water.

Briefly, the laser offers the advantage of depositing an extremely high energy on a small area of a target. This destructive energy is delivered at the speed of light (300 million meters per second which is ideal for a defensive system against missiles); whereas, a conventional missile travels to its target at a speed of a few times the speed of sound (roughly 1500 meters per second).

As alluded to earlier, beam quality has an important impact upon the overall laser system. Improvements in beam quality can be used to decrease overall laser size, shorten time for melting a metal, or decrease laser run time to perform a certain task. A well know fact is that beam quality depends on favorable illumination of the exit aperture; favorable illumination implies near constant phase and, to a lesser degree, near constant amplitude. Variation of the index of refraction within the cavity causes spatial variation in phase at the laser exit. This

nonuniform phase causes the peak axis intensity, I_{ff}, to
decrease according to

$$\frac{I_{ff}}{I_o} = \exp\ [-(2\pi\phi_{rms}/\lambda)^2]\ \tag{2}$$

where λ is wavelength. The rms phase, ϕ_{rms}, is obtained by
squaring and averaging the phase shifts across the aperture.
Equation (2) is the Strehle Ratio [21]. The spatial phase
relation is

$$\phi = \int nds \tag{3}$$

where ds is an incremental distance along a ray in the
laser cavity. The initial efforts to limit phase distortion
considered the index of refraction in terms of the Gladstone-
Dale formulation

$$.n = 1 + G\rho \tag{4}$$

where ρ is gas density, and G is the Gladstone-Dale constant;
hence there is concern for flow and acoustic effects. Hogge
and Crow [22] state that flow uniformity and reduced acoustic
effects have achieved $\Delta\rho/\rho = 5\times10^{-5}$, which is the required
flow uniformity.

It has been suggested, however, that the requirement for
flow uniformity should be stated in terms of $\Delta n/n$ due to
nonuniform pumping in the cavity [23]. In a typical flow
mixture, the constituents of the medium ($Ne:Xe:NF_3$) are

present in a fixed ratio (750:3:1) [24]. Even in a gas with fixed chemical composition, pressure and translational temperature, and hence, fixed $\Delta\rho/\rho$, $\Delta n/n$ can vary according to the ionic and electronic excitation of the medium caused by pumping.

Consider the Ladenburg formulation of the Kramers-Kronig dispersion relation [25]

$$n-1 = \frac{e^2 N}{2\pi m_e c^2} \sum_\ell \frac{N_\ell}{N} \sum_j \sum_k \frac{\lambda_{kj}^2 \, \lambda^2}{\lambda^2 - \lambda_{kj}^2} f_{kj} \left[1 - \frac{N_k g_j}{N_j g_k}\right] .$$

(5)

e   electron charge

c   speed of light

m_e mass of electron

N   total number

λ_{kj} wavelength for transition between k and j

λ wavelength of interest at which n is derived

f_{kj} is oscillator strength for transition from k to j

g_j is degeneracy of jth energy level

N_j population in j^{th} energy level

There are ℓ distinct species indicating specific electronic or ionic excitation present in the cavity. Index j sums over lower levels and k over upper levels of possible configurations. Identify the mole fraction as

$$X_\ell = \frac{N_\ell}{N} \tag{6}$$

the fraction of the total molecular population represented by species ℓ. Finally, define a quantity

$$T_\ell = \frac{e^2}{2\pi m_e c^2} \sum_j \sum_k \frac{\lambda_{kj}^2 \lambda^2}{\lambda^2 - \lambda_{kj}^2} f_{kj} \left[1 - \frac{N_k}{N_j} \frac{g_j}{g_k}\right] \tag{7}$$

In terms of the quantities defined above

$$n-1 = N \sum_\ell X_\ell T_\ell \tag{8}$$

or the index of refraction in the cavity is the sum of the contributions of all the species present in the cavity. Since $N_\ell = NX_\ell$,

$$n-1 = N_1 T_1 + N_2 T_2 + \dots \tag{9}$$

The partial density is given by $\rho_\ell = N_\ell m_\ell$ where m_ℓ is the molecular weight of ℓth species. In terms of partial density, equation (9) becomes

$$n-1 = \rho_1 T_1/m_1 + \rho_2 T_2/m_2 + \dots \tag{10}$$

Introduce the mass fraction for the gas mixture $Y_\ell = \rho_\ell/\rho$, where ρ is the density of the gas mixture. The result is

$$n-1 = \rho[Y_1 T_1/m_1 + Y_2 T_2/m_2 + \dots] \tag{11}$$

Equation (11) shows that n-1 is proportional to ρ; however, equation (11) further demonstrates that n-1 depends on mass fraction and index of refraction of each species. Even with uniform flow, the spatial phase relation across the cavity will not be uniform. Accurate modeling of the phase effects requires knowledge of the species populations and the contribution to the index of refraction of the species in the cavity. This thesis will explore a model for determining the species populations in a laser cavity and apply a model originally developed at the Naval Research Laboratory (NRL) to calculate the populations of the different configurations of excited Neon present in a XeF laser.

First, in section II, a review of electronic transition gas laser kinetics is discussed. Second, in section III, a simple model for an excimer (KrF) laser is developed. Third, in section IV, the computer program developed and written at NRL by Johnson, Palumbo, and Hunter [26] is discussed. Fourth, in section V, a formulation of input reactions to the NRL program to calculate the populations of excited neon configurations is developed. Fifth, in section VI, calculation of the index of refraction is performed. Sixth, in section VII, the calculation of phase shift is performed. Lastly, in section VIII, the results are discussed.

II. <u>KINETICS</u>

Electronic transition gas lasers (i.e. exciplex or
excimer) generally involve complex, branching chains of
energy flow from initial pump excitation of background gas
to eventual extraction of laser radiation. Figure 2 illus-
trates major energy flow pathways in e-beam pumped
$Ne/Xe/NF_3$ mixtures. These energy chains include processes
such as: energy deposition by electron ionization and
excitation; energy transfer by various collisional
mechanisms, including neutralization, displacement and
"harpooning", leading to formation of the upper laser
level; and collisional mechanisms which intercept excitation
energy before it can reach the upper laser level, or which
quench that level before stimulated emission occurs. Also,
one must consider extraction of stimulated emission includ-
ing absorptions by various processes in the gas and reso-
nant reabsorption by the lower laser level (if there is
one), laser cavity oscillation, and coupling through output
mirrors. A time-dependent model of the kinetics of such a
system must define and update species densities for a large
number--typically between 20 and 60--gas components, includ-
ing ground states, several excited states and ions of atoms
and molecules, plus electrons and photons.

The time evolution of these components is followed by
the solution of a set of coupled first order ordinary
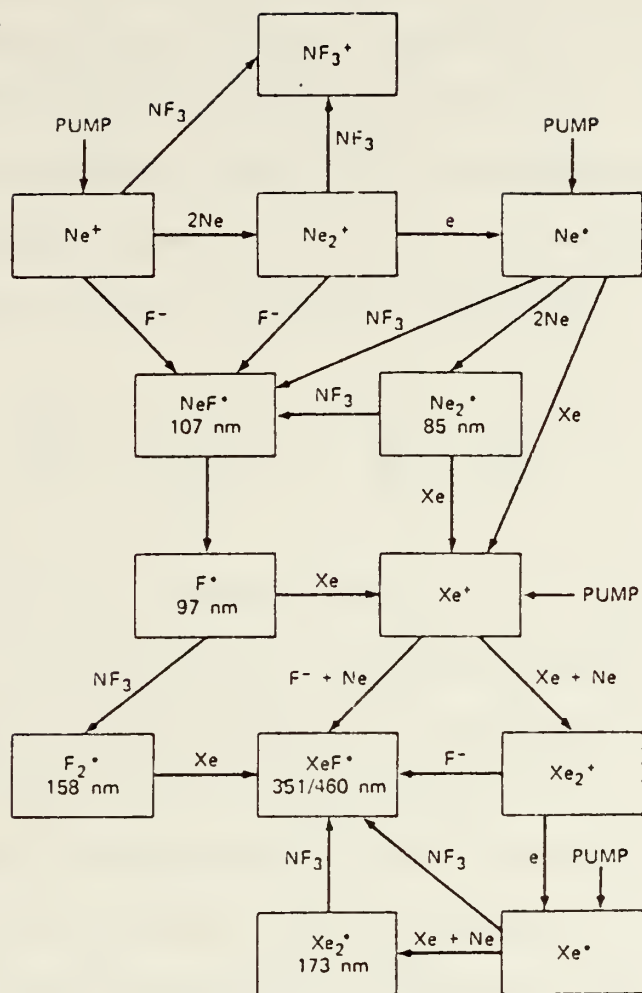
Figure 2. Major energy flow pathways in e-beam pumped
Ne/Xe/NF$_3$ mixtures (Reproduced from Huestis [27]).

Note: Energy input from the electrons comes in along
the pump arrows. The species in each box, plus
the component along the reaction arrow, yield
the result in the next box. The wavelengths of
the emitting species are indicated. They may be
subject to quenching by NF$_3$ or Xe (not shown).
NeF* is presumed to predissociate.

differential equations; one equation is required for each gas component. To the set of equations defining species densities are added further equations describing the evolution of the photon field, the gas temperature, and (in some models) coupled electrical circuit parameters. The species equations can be generally described as equating the rate of change of species density to a sum of contributing formation terms less a sum of depletion terms as

$$\frac{dN_i}{dt} = \sum_j F_{ji} - \sum_k D_{ik} \qquad (12)$$

Here N_i is a particular species density, the F_{ji} are the formation terms, and the D_{ik} the depletion terms. For example, consider a simple chemical reaction of the form $A + B \rightarrow C + D$ whose forward rate constant is k; if the species densities are expressed in cm^{-3}, the units of k are cm^3/sec. For this reaction, the rate equations defining species C and D would contain the formation term

$$F = k[A][B] ; \qquad (13)$$

at the same time, the equations defining species A and B would contain the depletion term

$$D = k[A][B] . \qquad (14)$$

Recall that square brackets for a chemical symbols means number density of the chemical with dimensions $1/cm^3$.

Consider equation (12) again. Species i is formed in j different reactions. Likewise, species i is depleted in k different reactions.

III. A SIMPLE KINETICS MODEL FOR KrF

In a thorough model of an excimer laser a large number
of kinetic reactions are necessary; see, for instance, the
185 reactions listed in the output of the NRL program for
XeF (Appendix A). The reactions are used to obtain the set
of coupled first order differential equations. The solution
to this set of equations is very involved and tedious
because of the difficulty in handling the tangle of reactions.
Therefore, only a few of the kinetic reactions in a KrF
laser are considered. The object of the simple computer
model was to obtain a qualitative insight to excimer laser
kinetics.

The model uses a $He/Kr/F_2$ mixture (98.1/1.77/0.13) with
He as diluent. Figure 3 illustrates a simplified e-beam
pumped KrF laser geometry.
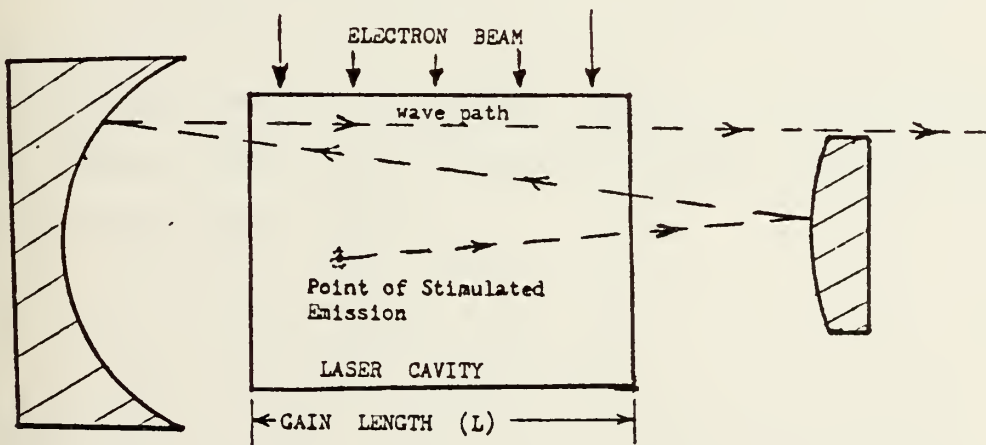
Figure 3. Example of e-beam pumped KrF laser geometry.

The first step in the kinetics chain leading to extraction of laser radiation is the deposition of energy in the diluent gas by either photons or electrons. In this model electrons are used. The electrons ionize the Kr and dissociate the F_2

$$e' + Kr \xrightarrow{k_1} Kr^+ + e + e' \qquad (15)$$
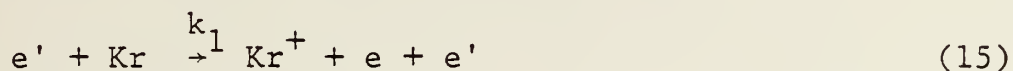
where e' is a primary electron, e is a secondary electron resulting from ionization of Kr, and k_1 is the forward rate constant. The secondary electron has sufficient energy to dissociate and electronegatively attach to atomic F.

$$e + F_2 \xrightarrow{k_2} F + F^- \qquad (16)$$
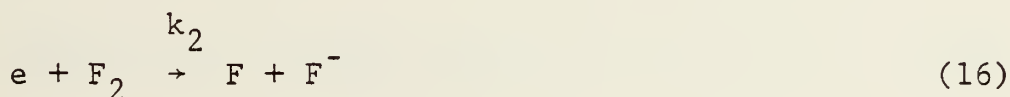
In addition dissociation of F_2 by the primary electrons occurs.

$$e' + F_2 \xrightarrow{k_3} F + F^- \qquad (17)$$

Having produced the ion pair states, recombination of positive rare gas ions and readily formed halide ions yields the excited state (KrF*).

$$Kr^+ + F^- + M \xrightarrow{k_4} KrF* + M \qquad (18)$$
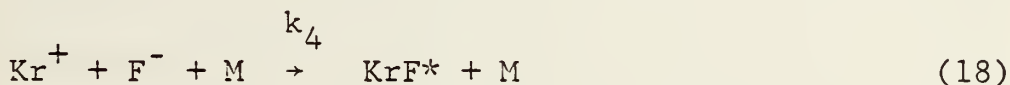
The KrF* can produce a photon by stimulated emission.

$$KrF* + h\nu \xrightarrow{k_5} KrF + 2h\nu \qquad (19)$$
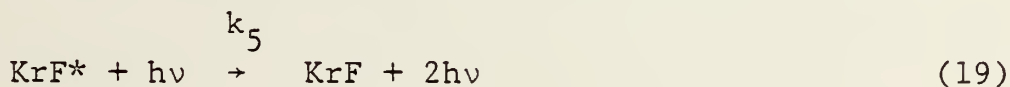
Also, recombination of F can occur

$$F + F + M \xrightarrow{k_6} F_2 + M \tag{20}$$
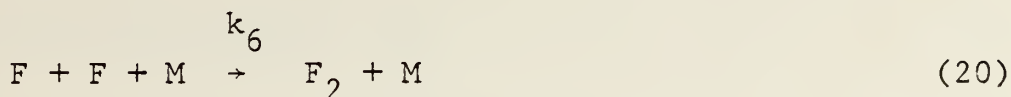
Fluorescence decreases KrF* population by

$$KrF* \xrightarrow{\tau} KrF + h\nu \tag{21}$$
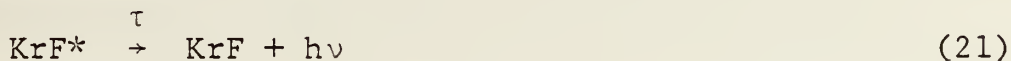
where τ is the radiative lifetime.

Reactions (15) to (21) are the only reactions considered in this model. None of the quenching processes of KrF* have been considered, such as

$$KrF* + 2Kr \xrightarrow{k} Kr_2F* + Kr \tag{22}$$
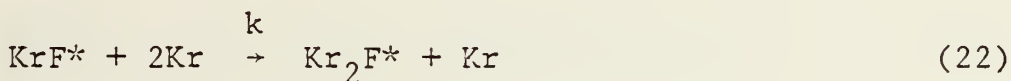
nor have many other reactions [2] and [28].

The reactions considered in this model are used to find the formation terms equation (13) and depletion terms equation (14). For example, examining reaction (15) the formation term for the concentration of e and Kr^+ is determined.

$$Formation \quad e = k_1[e'][Kr] \tag{23}$$

$$Formation \ Kr^+ = k_1[e'][Kr] \tag{24}$$

where [ ] denote concentration in specie number/cm^3.
The depletion term for concentration of e from reaction (16) is

Depletion $e = k_2[e][F_2]$ (25)

and for Kr^+ from reaction (18)

Depletion $Kr^+ = k_4[Kr^+][F^-][M]$ (26)

Applying equation (12), that is, equating the rate of change
of e concentration to the sum of contributing formation
terms equation (23) less the sum of depletion terms equation
(25) yields

$$\frac{d[e]}{dt} = k_1[e'][Kr] - k_2[e][F_2]$$ (27)

Similarly, combining equations (24) and (26)

$$\frac{d[Kr^+]}{dt} = k_1[e'][Kr] - k_4[Kr^+][F^-][M]$$ (28)

Continuing the process

$$\frac{d[F]}{dt} = k_2[e][F_2] + k_3[e'][F_2] - k_6[F][M]$$ (29)

$$\frac{d[F]}{dt} = k_2[e][F_2] + k_3[e'][F_2] - k_4[Kr^+][F^-][M]$$

(30)

$$\frac{d[KrF*]}{dt} = k_4[Kr^+][F^-][M] - k_5[h\nu][KrF*] - [KrF*]/\tau$$

(31)

$$\frac{d[KrF]}{dt} = k_5[KrF*][h\nu] + [KrF*]/\tau$$ (32)

are obtained.

In reaction (15) the e' is the e-beam input and there-
fore is a function of time. The model assumes the

concentration of e' is initially 1.0E13 electrons/cm^3 then becomes zero after about 177 nanoseconds. The secondary electron mean energy is 10 eV.

The rate constants (k) for the reactions were taken from scientific articles [2, 29, and 30] or derived as in the case of k_5. The values of the rate constants are listed in Table II. The radiative lifetime, τ, is equal to 15 nanoseconds from reference [2].

Table II. Rate Constants

Rate Constant	Value	Reference
k_1	5.0E-09 cm^3/sec	29
k_2	2.0E-09 cm^3/sec	30
k_3	5.0E-10 cm^3/sec	30
k_4	1.0E-25 cm^6/sec	2
k_5	1.5E-05 cm^3/sec	Derived in Appendix B
k_6	1.0E-31 cm^6/sec	2

Equations (27) to (32) can be solved to calculate the concentrations as a function of time. Multiplying these equations by dt yields a form for numerical solution on the HP9830. Equations (27) to (32) become

$$d[e] = (k_1[e'][Kr] - k_2[e][F_2])dt \qquad (33)$$

$$d[Kr] = (k_1[e'][Kr] - k_4[Kr^+][F^-][M])dt \qquad (34)$$

$$d[F] = (k_2[e][F_2] + k_3[e'][F_2] - k_6[F][M])dt \qquad (35)$$

$$d[F^-] = (k_2[e][F_2] + k_3[e'][F_2] - k_4[Kr^+][F^-][M])dt$$
$$\qquad (36)$$

$$d[KrF^*] = (k_4[Kr^+][F^-][M] - k_5[h\nu][KrF^*] - [KrF^*]/\tau)dt$$
$$\qquad (37)$$

$$d[KrF] = (k_5[KrF^*][h\nu] + [KrF^*]/\tau)dt \qquad (38)$$

respectively.

The initial conditions for the set of equations are:

$$[e] \quad = 0 \qquad\qquad\qquad\qquad\qquad\qquad\qquad\qquad (39)$$

$$[F] \quad = 0 \qquad\qquad\qquad\qquad\qquad\qquad\qquad\qquad (40)$$

$$[F^-] \quad = 0 \qquad\qquad\qquad\qquad\qquad\qquad\qquad\qquad (41)$$

$$[Kr^+] \quad = 0 \qquad\qquad\qquad\qquad\qquad\qquad\qquad\qquad (42)$$

$$[KrF] \quad = 0 \qquad\qquad\qquad\qquad\qquad\qquad\qquad\qquad (43)$$

$$[KrF^*] = 0 \qquad\qquad\qquad\qquad\qquad\qquad\qquad\qquad (44)$$

Several constants are specified as follows:

$$[h\nu] \quad = 4.0E11 \text{ (calculated in Appendix C)} \qquad (45)$$

$$[F_2] \quad = 4.0E16 \qquad\qquad\qquad\qquad\qquad\qquad\qquad (46)$$

Assumed values for

$$[Kr] \quad = 5.4E17 \quad \text{the He/Kr/}F_2 \text{ mixture} \qquad\qquad (47)$$

(93.1/1.77/0.13) at

$$[He] \quad = 3.0E19 \quad \text{STP.} \qquad\qquad\qquad\qquad\qquad (48)$$

Initial T = 0

Final T = 250 nanoseconds

Delta T = (Final T - Initial T)/256

A computer program was written using equations (33) to (38) and the initial conditions and appropriate constants given by equations (39) to (48). Figures 4 and 5, which are plots obtained from the HP9830 program, are the concentrations

in specie number/cm^3 versus time from 0 to 250 nanoseconds.
The plots in Figures 4 and 5(b) indicate that some species
densities rise extremely steeply in the first tenth of the
simulation time; later in the pulse (after about 50 nano-
seconds) species densities tend to flatten out. See Figure 4.
Once the e-beam terminates, the decay time is approximately
50 nanoseconds. In Figure 5(a) and (b) other species
densities increase gradually and flatten out. The results
of this model are in qualitative agreement with the NRL
simulation contained in reference [26]. The NRL simulation
limited the change in concentration to 5 percent per time-
step to obtain sufficient accuracy [26]. The question of
timesteps for the simple model was avoided; sufficiently
small steps were used throughout the program.

Table III lists the variables, symbols, and equations
used in HP9830 computer program.

Table IV lists the KrF Computer Program and Table V
lists the output.
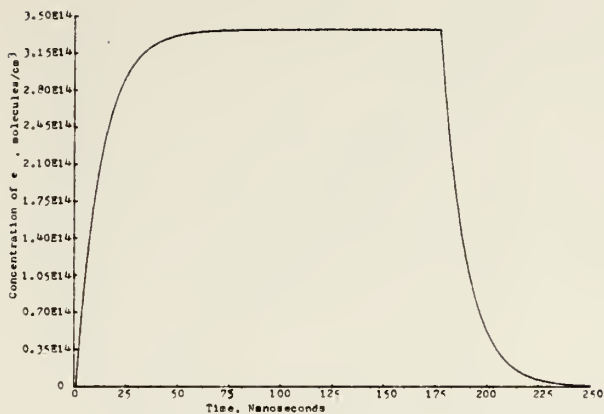
(a)   Concentration of secondary electrons
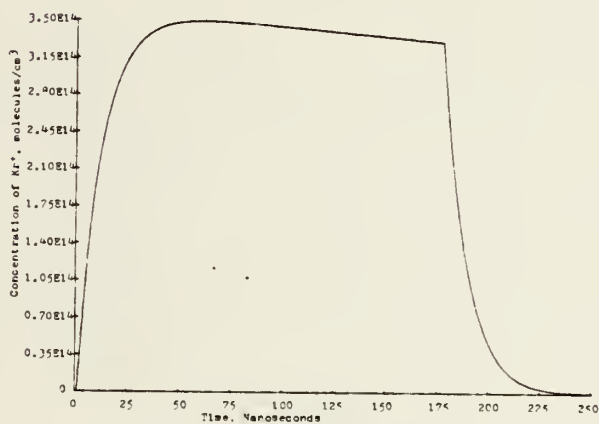
(b)   Concentration of Kr^+
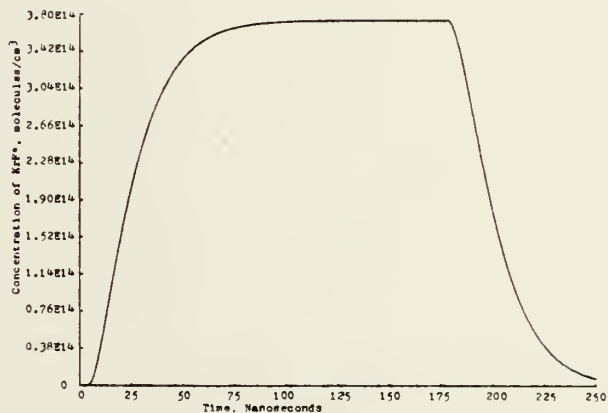
(c)   Concentration of KrF*

Figure 4.   Concentration of secondary electrons (e), Kr^+ and KrF*, molecules/cm^3, as a function of time.
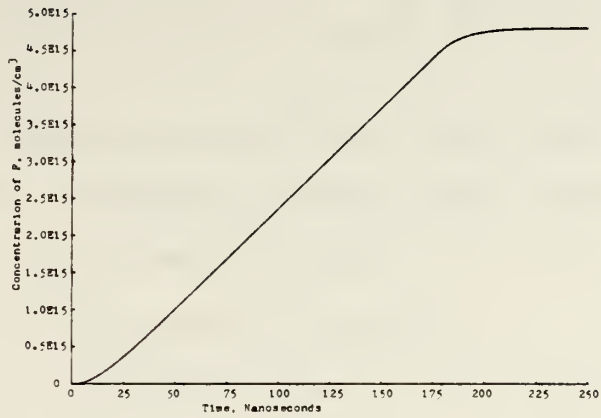
(a)   Concentration of F
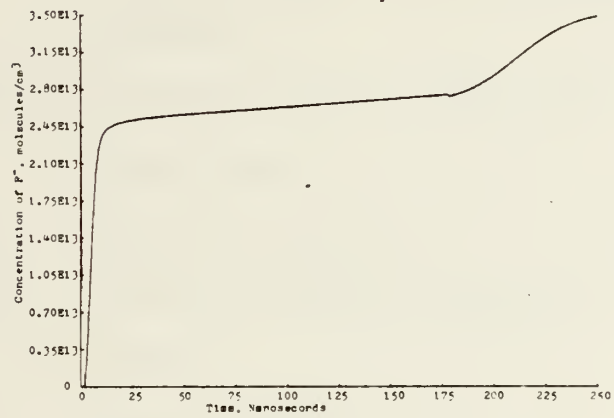
(b)   Coneentration of F⁻
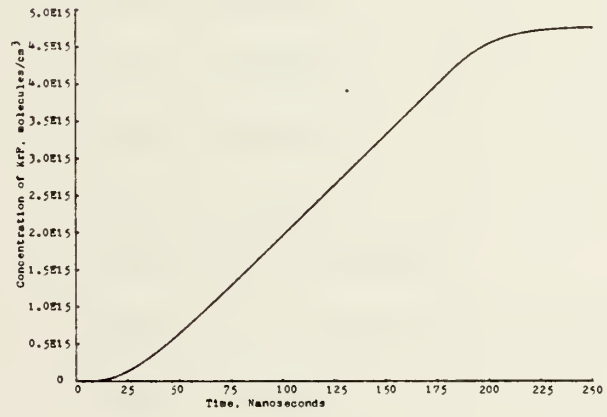
(c)   Concentration of KrF

Figure 5.   Concentration of F, F⁻, and KrF molecules/cm³, as a function of time.

Table III. Variables, Symbols, and Equations Used in
HP9830 Computer Program for KrF Laser.

Variables and Symbols Used in the Program

HP9830	Text	Meaning or Value (for constants)	Units
El	e'	primary electron	-
E	e	secondary electron	-
F	F	Fluorine atom	-
G	F_2	Fluorine molecule	-
H	F^-	Fluorine atom with extra electron	-
K	Kr	Krypton	-
L	Kr^+	Krypton minus an electron	-
M	M	Third body	-
X	KrF	Krypton Fluoride	-
Y	KrF*	Krypton Fluoride excited	-
P	$h\nu$	photon	joules
K1	k_1	Rate constant	cm^3/sec
K2	k_2	Rate constant	cm^3/sec
K3	k_3	Rate constant	cm^3/sec
K4	k_4	Rate constant	cm^6/sec
K5	k_5	Rate constant	cm^3/sec
K6	k_6	Rate constant	cm^6/sec
T1	τ	Radiative lifetime	sec
I	-	Index; I=1 for initial conditions	-
T	t	Time increment	sec

Table III (Continued). Variables, Symbols, and Equations
          Used in HP9830 Computer Program for KrF Laser.

Equations Used in the Program

Line Number	Equation Number
860	33
870	34
880	35
890	36
900	45
910	37
920	38

```
10 FORMAT 7E10.3
20 DIM EC256],FC256],HC256],LC256],YC256],XC256],XLC256]
30 DIM GC256],AC256],KC256],MC256],PC256]
40 PRINT "PROGRAM FOR COUPLED KINETIC EQUATIONS FOR THREE ELEMENT GAS LASER"
50 PRINT ": * * * * * * * * * * * * * * * * * * * * * * * * * *"
60 PRINT ": THIS PROGRAM IS FOR HP9830."
70 PRINT ": A PRIMARY ELECTRON"
80 PRINT ": E SECONDARY ELECTRON"
90 PRINT ": F FLUORINE"
100 PRINT ": G FLUORINE SUB 2"
110 PRINT ": H FLUORINE MINUS"
120 PRINT ": K KRYPTON"
130 PRINT ": L KRYPTON PLUS"
140 PRINT ": M THIRD BODY (DILUENT E.G. HELIUM)"
150 PRINT ": X KRYPTON FLUORIDE"
160 PRINT ": Y KRYPTON FLUORIDE EXCITED"
170 PRINT ": P PRODUCT (PLANCK'S CONSTANT)*(FREQUENCY)"
180 PRINT ": RATE CONSTANTS  K1,K2,K3,K4,K5,K6"
190 T2=0
200 Z=0
210 PRINT "INPUT INITIAL CONDITIONS"
220 GOTO 950
570 DISP "T INITIAL=";
580 INPUT S
590 DISP "T FINAL =";
600 INPUT S9
610 S1=(S9-S)/256
620 T=S1
630 PRINT "EC1]="EC1],"FC1]="FC1],"HC1]="HC1],"LC1]="LC1],"XC1]="XC1]
640 PRINT "YC1]="YC1],"PC1]="PC1],"GC1]="GC1]
650 PRINT "KC1]="KC1],"MC1]="MC1]
660 PRINT "AC1],"T1(RADIATIVE LIFETIME)="T1
670 PRINT "K1="K1,"K2="K2
680 PRINT "K3="K3,"K4="K4
```

Table IV.   Listing of the HP9830 KrF Program

```
690 PRINT "K5="K5,"K6="K6
700 PRINT ;"INITIAL T=";S,"FINAL T=";S9
705 PRINT ;"DELTA T=";T
710 PRINT
720 PRINT "CONCENTRATIONS AT TIME (T)"
730 PRINT "   TIME   E(SECONDARY) F    .F-      KR+      KRF*     KRF"
731 PRINT
735 WRITE (15,10)S,E[1],F[1],H[1],L[1],Y[1],X[1]
736 PRINT
740 FOR I=1 TO 256
750 IF I=256 THEN 1130
760 A[I]=A[1]
770 K[I]=K[1]
780 G[I]=G[1]
800 M[I]=M[1]
810 Z=Z+1
820 R=INT(Z/10)
830 V=ABS(R-Z/10)
840 IF V#0 THEN 860
850 WRITE (15,10)T2,E[1],F[1],H[1],L[1],Y[1],X[1]
855 PRINT
860 E[I+1]=E[I]+(K1*H[I]*K[I]-K2*E[I]*G[I])*T
870 F[I+1]=F[I]+(E[I]*G[I]*K2+A[I]*G[I]*K3-K6*F[I]↑2*M[I])*T
880 H[I+1]=H[I]+(K2*E[I]*G[I]+K3*A[I]*G[I]-K4*L[I]*H[I])*T
890 L[I+1]=L[I]+(K1*K[I]*H[I]-K4*L[I]*H[I]*M[I])*T
900 P[I]=P[1]
910 Y[I+1]=Y[I]+(K4*L[I]*H[I]*M[I]-K5*P[I]*Y[I]-Y[I]/T1)*T
920 X[I+1]=X[I]+(K5*Y[I]*P[I]+Y[I]/T1)*T
930 T2=T2+T
935 IF I>180 THEN 941
940 NEXT I
941 A[1]=0
942 GOTO 940
950 E[1]=0
```

Table IV (Continued). Listing of the HP9830 KrF Program

35

```
960 F[1]=0
970 H[1]=0
980 L[1]=0
990 X[1]=0
1000 Y[1]=0
1010 P[1]=4E+11
1020 G[1]=4E+16
1030 K[1]=5.4E+17
1040 M[1]=3E+19
1050 A[1]=1E+13
1055 T2=0
1060 T1=1.5E-08
1070 K1=5E-09
1080 K2=2E-09
1090 K3=5E-10
1100 K4=1E-25
1110 K5=1.5E-05
1115 K6=1E-31
1120 GOTO 570
1130 DISP "INPUT T9";
1140 INPUT T9
1150 DISP "INPUT C9";
1160 INPUT C9
1170 SCALE 0,T9,0,C9
1180 XAXIS 0,T9/10
1190 YAXIS 0,C9/10
1200 FOR I=1 TO 256
1210 T8=I*T
1220 PLOT T8,X[I]
1230 NEXT I
1240 PEN
1250 PRINT "CONT 1150"
1260 PRINT
1270 STOP
1350 END
```

Table IV (Continued). Listing of the HP9830 KrF Program

36

```
PROGRAM FOR COUPLED KINETIC EQUATIONS FOR THREE ELEMENT GAS LASER
* * * * * * * * * * * * * * * * * * * * * * * * * * * * * * * * * *
THIS PROGRAM IS FOR HP9830
A   PRIMARY ELECTRON
E   SECONDARY ELECTRON
F   FLUORINE
G   FLUORINE SUB 2
H   FLUORINE MINUS
K   KRYPTON
L   KRYPTON PLUS
M   THIRD BODY (THE DILUENT
X   KRYPTON FLUORIDE
Y   KRYPTON FLUORIDE EXCITED
P   PRODUCT (PLANCK'S CONSTANT)*(FREQUENCY)
RATE CONSTANTS  K1,K2,K3,K4,K5,K6
INPUT INITIAL CONDITIONS
E(1)= 0            F(1)= 0            H(1)= 0            L(1)= 0            X(1)= 0
Y(1)= 0            P(1)= 4.00000E+11                     G(1)= 4.00000E+16
K(1)= 5.40000E+17                     M(1)= 3.00000E+19
A(1)= 1.00000E+13                     T1(RADIATIVE LIFETIME)= 1.50000E-08
K1= 5.00000E-09                       K2= 2.00000E-09
K3= 5.00000E-10                       K4= 1.00000E-25
K5= 1.50000E-05                       K6= 1.00000E-31
INITIAL T= 0                          FINAL T= 2.50000E-07
DELTA T= 9.76563E-10
```

Table V. Output of the HP9830 KrF Program

37

CONCENTRATIONS AT TIME (T)

TIME	E(SECONDARY)	F	F-	KR+	KRF*	KRF
0.000E+00	0.000E+00	0.000E+00	0.000E+00	0.000E+00	0.000E+00	0.000E+00
8.789E-09	1.752E+14	6.386E+13	2.322E+13	1.967E+14	3.632E+13	4.318E+12
1.855E-08	2.655E+14	2.391E+14	2.487E+13	2.067E+14	1.482E+14	6.605E+13
2.832E-08	3.056E+14	4.647E+14	2.524E+13	3.252E+14	2.378E+14	2.017E+14
3.809E-08	3.234E+14	7.126E+14	2.545E+13	3.412E+14	2.963E+14	3.908E+14
4.785E-08	3.312E+14	9.703E+14	2.561E+13	3.473E+14	3.313E+14	6.134E+14
5.762E-08	3.347E+14	1.232E+15	2.576E+13	3.490E+14	3.512E+14	8.555E+14
6.738E-08	3.363E+14	1.496E+15	2.589E+13	3.487E+14	3.621E+14	1.109E+15
7.715E-08	3.370E+14	1.761E+15	2.603E+13	3.476E+14	3.679E+14	1.368E+15
8.691E-08	3.373E+14	2.027E+15	2.617E+13	3.460E+14	3.709E+14	1.630E+15
9.668E-08	3.374E+14	2.292E+15	2.631E+13	3.444E+14	3.725E+14	1.894E+15
1.064E-07	3.375E+14	2.557E+15	2.645E+13	3.426E+14	3.733E+14	2.158E+15
1.162E-07	3.375E+14	2.823E+15	2.659E+13	3.408E+14	3.737E+14	2.423E+15
1.260E-07	3.375E+14	3.088E+15	2.673E+13	3.390E+14	3.739E+14	2.688E+15
1.357E-07	3.375E+14	3.353E+15	2.687E+13	3.372E+14	3.740E+14	2.954E+15

Table V (Continued). Output of the HP9830 KrF Program

1.455E-07	3.375E+14	3.619E+15	2.702E+13	3.354E+14	3.741E+14	3.219E+15
1.553E-07	3.375E+14	3.884E+15	2.716E+13	3.336E+14	3.741E+14	3.485E+15
1.650E-07	3.375E+14	4.149E+15	2.731E+13	3.318E+14	3.741E+14	3.750E+15
1.748E-07	3.375E+14	4.414E+15	2.746E+13	3.300E+14	3.741E+14	4.016E+15
1.846E-07	1.761E+14	4.628E+15	2.773E+13	1.684E+14	3.300E+14	4.274E+15
1.943E-07	7.805E+13	4.725E+15	2.863E+13	7.133E+13	2.259E+14	4.475E+15
2.041E-07	3.460E+13	4.768E+15	2.993E+13	2.918E+13	1.376E+14	4.606E+15
2.139E-07	1.534E+13	4.787E+15	3.142E+13	1.141E+13	7.828E+13	4.683E+15
2.236E-07	6.000E+12	4.795E+15	3.281E+13	4.254E+12	4.246E+13	4.726E+15
2.334E-07	3.015E+12	4.798E+15	3.386E+13	1.523E+12	2.223E+13	4.749E+15
2.432E-07	1.337E+12	4.799E+15	3.455E+13	5.301E+11	1.133E+13	4.761E+15

Table V (Continued). Output of the HP9830 KrF Program

IV. XeF LASER COMPUTER PROGRAM FROM NRL

In order to calculate the excited states of neon in a XeF laser a complex kinetics program is required. A kinetics scheme for the XeF laser developed at the Naval Research Lab was used. It was written by Dr. Louis J. Palumbo [26 and 31] who assisted greatly in modifying it for use on the IBM 360/67.

The computer model consists of two parts: first, an e-beam deposition section, in which the kinetic energy of near relativistic electrons is used to ionize and excite the laser gas, and, second, a chemical kinetics section, in which the energy deposited in the gas cascades down by various processes to the upper laser level and is extracted as laser radiation.

One input to the NRL computer model is a list of reactions, e.g. in the format of equations (16) to (21). Also an input is a list of reaction rate coefficients. The computer program sorts the reactions and forms formation terms, F, and depletion terms, D. Formation and depletion terms were discussed earlier in connection with equations (13) and (14). Continuing, the computer program selects the appropriate F and D terms to form the rate equation of equation (12). Next, the computer program multiplies the rate equation by a variable timestep. The same approach was used in the simple computer program; see equations (33) to (38).

An advantage of the NRL program is the ability to change
the number of reactions. The computer program does not change;
only the input changes. The differential equations are
generated internal to the program. This method makes it much
easier to alter the set of equations and greatly reduces errors
attendant to such alterations which arise with ease in the
complex tangle of reactions. The detailed explanation of the
computer model is contained in references [26] and [31].
Appendix A gives a list of reactions used to generate the
population distribution within neon energy levels.

V. CALCULATION OF NEON EXCITED
STATE POPULATIONS

The excited states of neon are represented in Figure 6. The electronic configurations of interest to this study are the 3s, 3p, 4s, 3d, 4p, 5s, 4d, 4f, 5p, 5d, and 6s.

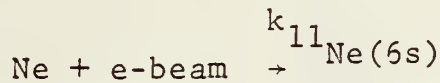In order to calculate the populations of these particular configurations, one needs to know the reactions involved and the rate constants. For example,

$$Ne + e\text{-beam} \xrightarrow{k_1} Ne(3s)$$

$$Ne + e\text{-beam} \xrightarrow{k_2} Ne(3p)$$

$$\ldots$$

$$Ne + e\text{-beam} \xrightarrow{k_{11}} Ne(6s)$$
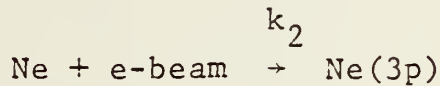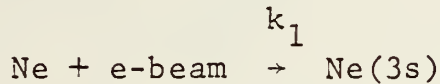
These reactions could then be input to the NRL XeF program to calculate the populations of the excited configurations of neon. After, an extensive literature search (Optics and Spectroscopy, The Journal of Chemical Physics, Applied Physics Letters, Physical Review A, Journal of the Optical Society of America, Chemical Abstracts, IEEE Journal of Quantum Electronics, etc.) rate constants for the individual excited configurations i.e. 3s, 3p, ... were not found.

Therefore, it was necessary to make a number of assumptions. The procedure followed was to extract all reactions
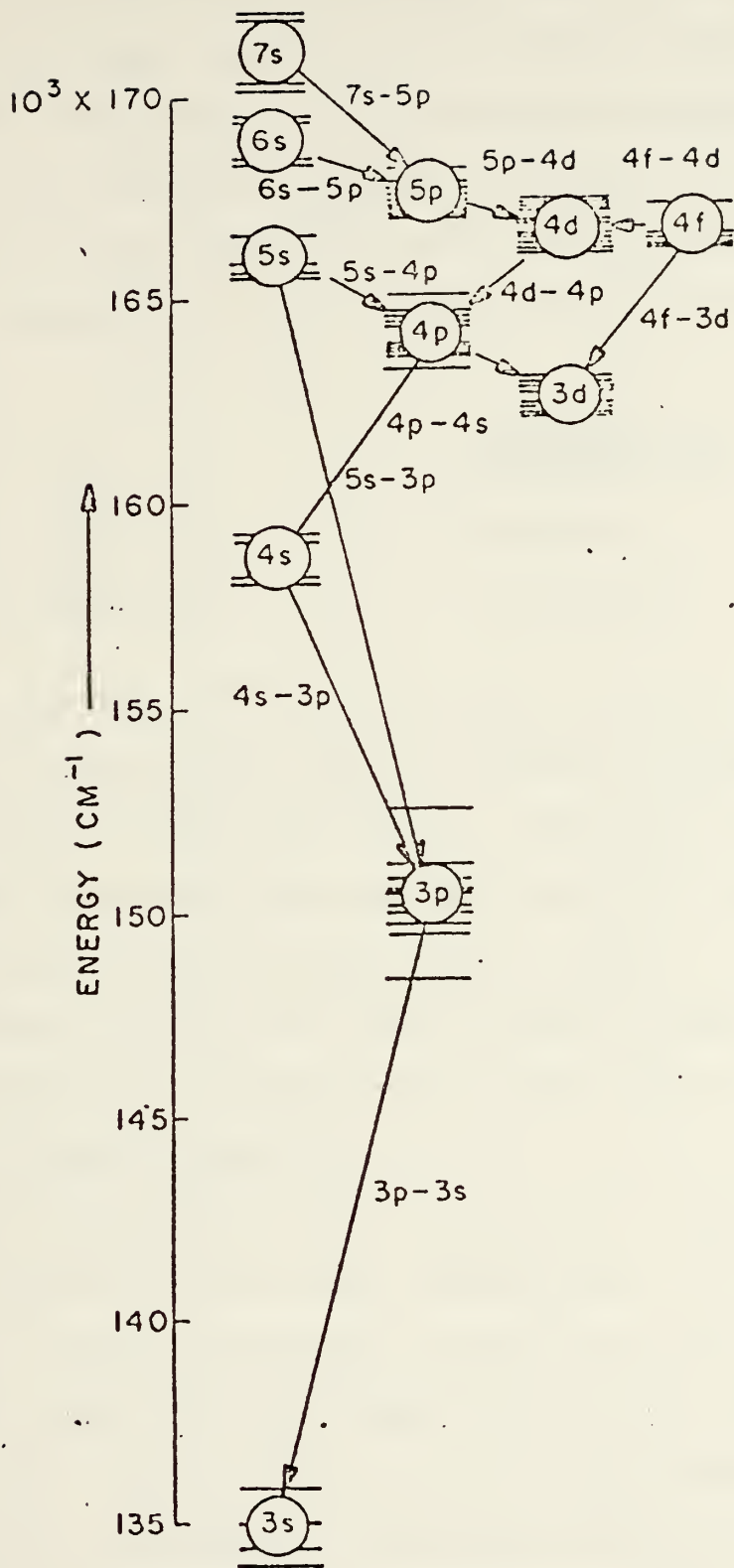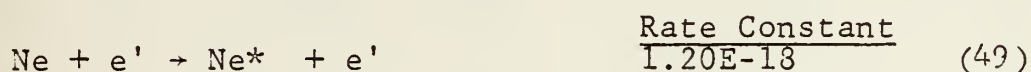
Figure 6. Energy-Level diagram of Neon (Reproduced from Pressley [32].

from the NRL program involving the neon excited state (Ne*).
Then, these reactions were subdivided into two groups, the
Ne(3s) and all higher configurations, which are denoted by
NE*1 and NE*Z respectively. The population distribution
within NE*Z was calculated assuming a Boltzmann distribution.

The list of reactions which were used as modified input
to the NRL program are listed in Table VI in the following
format:

		Rate Constant	
Ne + e' → Ne* + e'		1.20E-18	(49)
Ne + e' → Ne*1 + e'		0.925E-18	(50)
Ne + e' → Ne*Z + e'		0.275E-18	(51)

To compare equations (49) to (51) with the first three
reactions of Table VI note that e' is EBEM in FORTRAN nota-
tion. The other symbols are obvious. The first reaction
yielding Ne* is divided into the Ne*1 and Ne*Z reactions.
A computer run with the current density equal to 10 A/cm^2
and a computer run with the current density equal to 11
A/cm^2 calculated the populations for Ne*1 (3s) and Ne*Z
(all levels greater than 3s).

The rate constants for the reactions were determined by
taking a fraction of the total rate constant. For example,
in Table VI, for the second set of reactions, the rate
constant for NE*1 is 0.8 and NE*Z is 0.2 of the rate con-
stant for NE*. These fractions of the rate constant for
NE* are noted in parentheses following the reactions. The
choices of the fractional values were arbitrary.

TABLE VI. Input Reactions to the NRL Program.[*]

Reaction							Rate Constant
NE	+ EBEM	→ NE*	+ EBEM				1.20 E-18
NE	+ EBEM	→ NE*1	+ EBEM				0.925E-18
NE	+ EBEM	→ NE*Z	+ EBEM				0.275E-18
NE*	+ E-	→ NE	+ E-				2.00 E-10
NE*1	+ E-	→ NE	+ E-			(.8)	1.60 E-10
NE*Z	+ E-	→ NE	+ E-			(.2)	0.40 E-10
NE2+	+ E-	→ NE*	+ NE				3.50 E-08
NE2+	+ E-	→ NE*1	+ NE			(.9)	3.15 E-08
NE2+	+ E-	→ NE*Z	+ NE			(.1)	0.35 E-08
NE3+	+ E-	→ NE*	+ NE	+ NE			3.50 E-08
NE3+	+ E-	→ NE*1	+ NE	+ NE		(.95)	3.325E-08
NE3+	+ E-	→ NE*Z	+ NE	+ NE		(.05)	0.175E-08
XENE+	+ E-	→ NE*	+ XE				6.00 E-08
XENE+	+ E-	→ NE*1	+ XE			(.6)	3.60 E-08
XENE+	+ E-	→ NE*Z	+ XE			(.4)	2.40 E-08
NE*	+ NE + NE	→ NE2*	+ NE				5.0 E-34
NE*1	+ NE + NE	→ NE2*	+ NE			(.8)	4.0 E-34
NE*Z	+ NE + NE	→ NE2*	+ NE			(.2)	1.0 E-34
NE*	+ XE	→ XE+	+ E-	+ NE			7.40 E-11
NE*1	+ XE	→ XE+	+ E-	+ NE		(.6)	4.44 E-11
NE*Z	+ XE	→ XE+	+ E-	+ NE		(.4)	2.96 E-11
NE*	+ XE	→ NEXE+	+ E-				2.20 E-11
NE*1	+ XE	→ NEXE+	+ E-			(.6)	1.32 E-11
NE*Z	+ XE	→ NEXE+	+ E-			(.4)	0.88 E-11

TABLE VI (Continued). Input Reactions to the NRL Program.[*]

Reaction					Rate Constant
NE* + F2	→ NEF*	+ F			4.10 E-10
NE*1 + F2	→ NEF*	+ F	(.8)		3.28 E-10
NE*Z + F2	→ NEF*	+ F	(.2)		0.62 E-10
NE* + NF3	→ NEF*	+ NF2			1.05 E-10
NE*1 + NF3	→ NEF*	+ NF2	(.8)		0.84 E-10
NE*Z + NF3	→ NEF*	+ NF2	(.2)		0.21 E-10
NE* + NF2	→ NEF*	+ NF			1.0 E-10
NE*1 + NF2	→ NEF*	+ NF	(.8)		0.8 E-10
NE*Z + NF2	→ NEF*	+ NF	(.2)		0.2 E-10
NE* + NF	→ NEF*	+ N			1.0 E-10
NE*1 + NF	→ NEF*	+ N	(.8)		0.8 E-10
NE*Z + NF	→ NEF*	+ N	(.2)		0.2 E-10
NE2* + HN352L	→ NE*	+ NE + ABSL			1.0 E-18P
NE2* + HN352L	→ NE*	+ NE + ABSL	(.9)		0.9 E-18P
NE2* + HN352L	→ NE*	+ NE + ABSL	(.1)		0.1 E-18P

[*]Use of capital letters more closely represents computer printing.

However, the first reactions listed in Table VI do not have fractional values in parentheses, as the reaction rate constants were determined using reference [9]. The plot of "Excitation of Neon by Electrons" from page 467 of reference [9] was extrapolated to 10 keV, and the value for the $2p_1$ state was assumed to represent all excited configurations above the 3s (NE*1). The difference between the rate constant for NE* and the $2p_1$ value yielded the rate constant for NE*1.
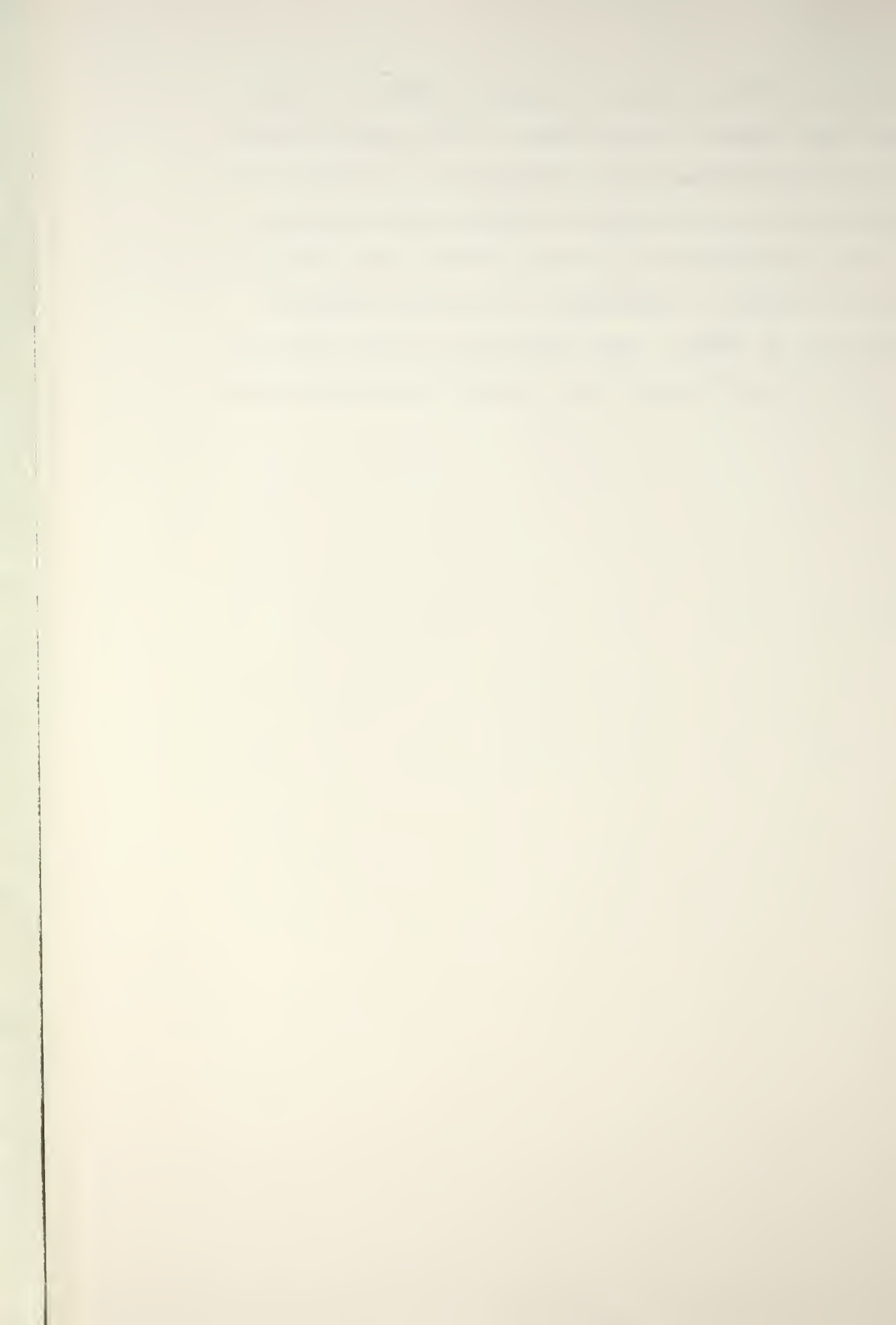
VI. CALCULATION OF THE INDEX OF REFRACTION

The values (n-1)/N where n is the index of refraction and N is the species population, have been calculated Refs. [33], [34] and [35]. Figure 7 lists the values of (n-1)/N. References [34] and [35] contain the details of calculating these values.

The index of refraction (n-1) is equal to

$$n-1 = (\frac{(n-1)}{Ne}) \; N + (\frac{n-1}{Ne(3s)}) \; N(3s) + (\frac{n-1}{Ne(Z)}) \; N(Z) \quad (52)$$
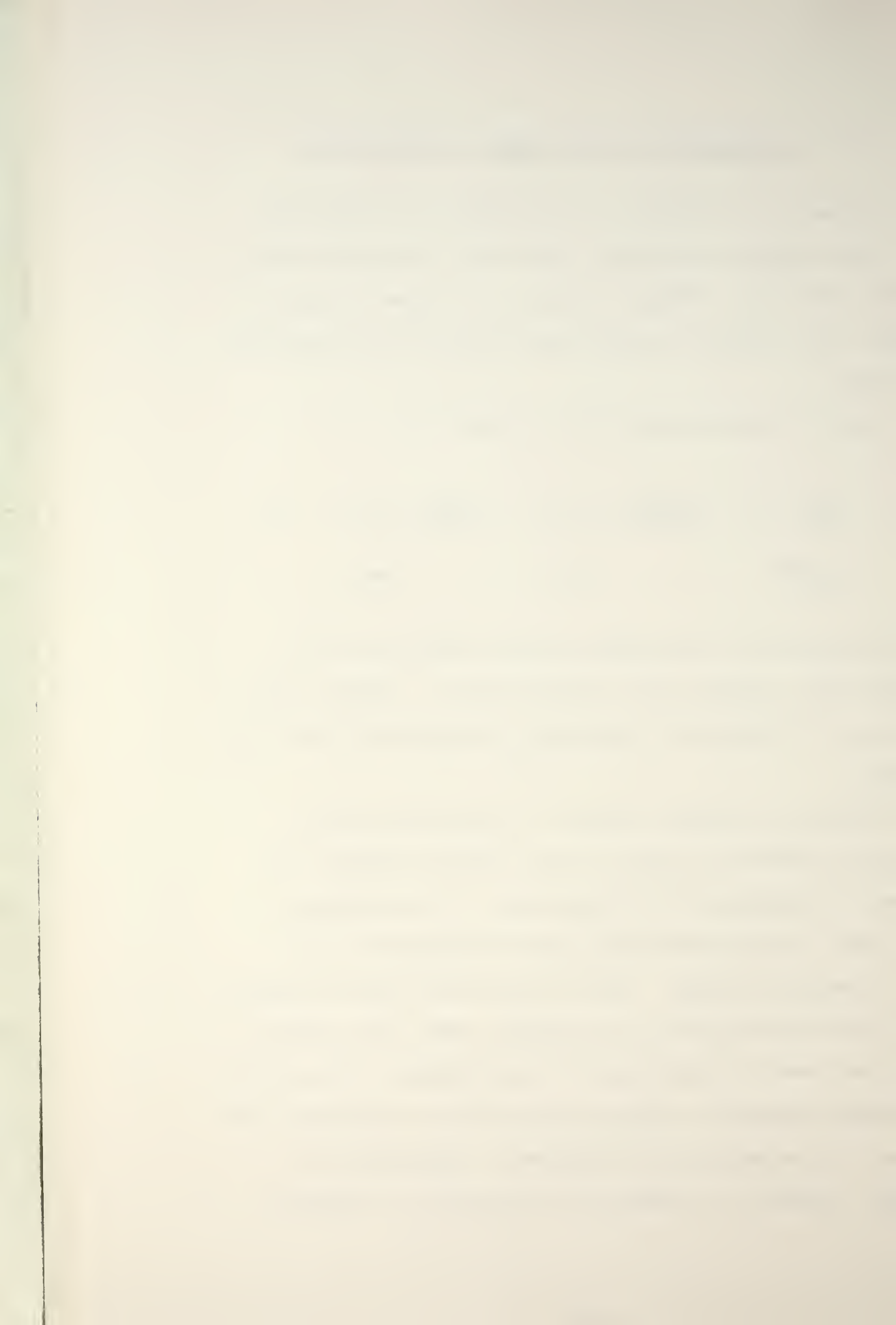
$$\text{ground} \qquad\qquad\qquad Ne*1 \qquad\qquad\qquad Ne*Z$$
$$\text{state}$$

Using the populations calculated in the NRL model for N, N(3s), and N(Z) equation (52) can be solved. However, the populations of individual electronic configurations must be determined.

One feature of excimer lasers, in contrast to the vibrational transition lasers of the infrared region, is the extent of randomness of populations. In the CO_2 gas dynamic laser, mode temperatures can be assigned to the various vibrational modes. Due to the short span of excitation and power extraction in an excimer laser, the various modes do not have an opportunity to equilibrate. This fact is the reason extensive computer programs are necessary for kinetics. An assumption of a Boltzmann distribution is unfounded. However, in view of the sparsity of reaction

Figure 7. Matrix of significant configuration arrays. The number in the blocks is (n-1)/N cm³ multiplied by 10²⁷ (Reproduced from Fuhs, Etchechury, and Cole [33]).

R^ resonance - requires special attention

rate coefficients for excitation to specific configurations
a Boltzmann distribution is assumed. Assuming a Boltzmann
relation for the upper levels the populations of the 3p,
4s, 3d, ... 6s can be calculated.

$$N(Z) = N(3p) + N(4s) + N(3d) + \ldots + N(6s) \qquad (53)$$

$$N(Z) = N(3p) \left[1 + \frac{g_{4s}}{g_{3p}} \exp^{\frac{-(E_{4s}-E_{3p})}{kT}} + \frac{g_{3d}}{g_{3p}} \exp^{\frac{-(E_{3d}-E_{3p})}{kT}} \ldots \right] \qquad (54)$$

where g denotes the degeneracy of the configuration which is
equal to the sum of the 2J + 1 terms. E is the energy sub-
scripted by the configuration.

Solving for N(3p)

$$N(3p) = \frac{N(Z)}{1 + \frac{g_{4s}}{g_{3p}} \exp^{\frac{-(E_{4s}-E_{3p})}{kT}} + \ldots} \qquad (55)$$

All the quantities on the right side of equation (55)
are known or can be calculated. Table VII lists the values
of the degeneracies and energies for the configurations.

TABLE VII. Degeneracy and energy values for the configurations.

Electronic Configuration	g(Σ 2J +1)	E (cm^{-1})
3s	12	134674.6
3p	36	150197.8
4s	12	158950.1
3d	73	161874.4
4p	36	163180.3
5s	12	166123.2
4d	73	166500
4f	84	166562
5p	36	167812.5
5d	73	168000 .
6s	12	168750

The temperature T is calculated as follows using the Boltzmann relation

$$\frac{N(3s)}{N(2p)} = \frac{g_{3s}}{g_{2p}} \exp \frac{-(E_{3s}-E_{3p})}{kT} \tag{56}$$

Solving for T

$$\ln \left[\frac{N(3s)}{N(2p)} \frac{g_{2p}}{g_{3s}} \right] = \frac{-(E_{3s}-E_{2p})}{kT}$$

$$T = \frac{-(E_{3s} - E_{2p})}{k \ln \left[\frac{N(3s)}{N(2p)} \frac{g_{2p}}{g_{3s}} \right]} \tag{57}$$

Substituting the value of T into equation (55) yields a value for N(3p). To calculate N(4s) one uses

$$N(4s) = N(3p) \frac{g_{4s}}{g_{3p}} \exp \left[\frac{-(E_{4s} - E_{3p})}{kT} \right] \tag{58}$$

Similarly the populations of the other configurations can be calculated i.e. N(3d), N(4p), etc. Once the populations of the configurations have been found it is a simple calculation to obtain n-1 applying equation (52) as

$$\frac{n-1}{Ne(3p)} \; , \; \frac{n-1}{Ne(4s)} \; , \; \cdots \; \frac{n-1}{Ne(5s)}$$

are given along the bottom of Figure 7.

A computer program to calculate the index of refraction (n-1) using equations (52), (55), (57), and (58) was written.

In Figure 7 the 3s → 4p transition contains an R*. R* indicates that resonance may occur and can have a large effect on the index of refraction. The spikes in Figure 8 are located at the resonant wavelengths. Resonance is discussed in reference [36].
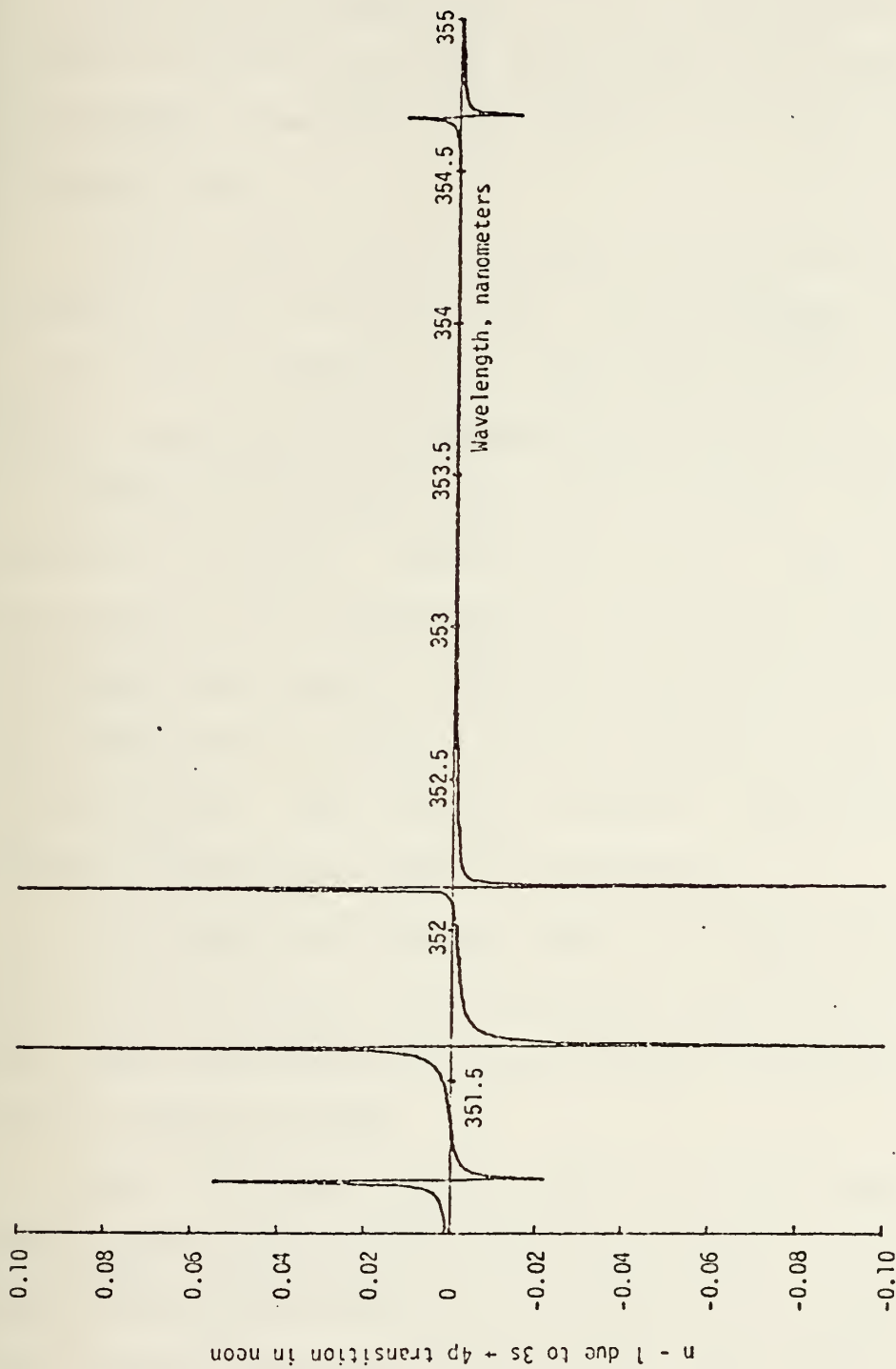
Figure 8. Plot of n-1 as a function of wavelength. The quantity plotted is contribution of 3s → 4p transition in neon (Reproduced from Fuhs, Etchechury, and Cole [36]).

The plots in Figure 9 are of the calculated indices of refraction (n-1) versus time (nanoseconds). Figure 9(a) is for a laser wavelength away from 3s → 4p (no resonance) for both low and high power. The current density for low power is 10 A/cm^2, and the high power is 11 A/cm^2. For a nonresonant wavelength, the change in n-1 is in the fourth decimal place.

The resonance effect was taken into account in a second computer run; see Figure 9(b). For a resonant laser wavelength, the contribution to the index of refraction due to Ne(3s) was calculated assuming (n-1)/Ne(3s) equal to -5.0E08; the corresponding value for Ne(4p) was (n-1)/Ne(4p) equal to 1.667E08. Figure 9(b) is for a laser wavelength near the 3s → 4p resonance for low and high power. The resonance has a marked effect on the index of refraction in comparison to Figure 9(a) as evidenced by the ordinates of the plots. Also, Figure 9 reveals that increasing the power decreases the index of refraction.

The right hand ordinate scale for Figure 9(a) is the ratio (n-1)/(n-1)$_o$, where (n-1)$_o$ is the value at zero time. The scale emphasizes the fact that the relative changes are in the fourth decimal.
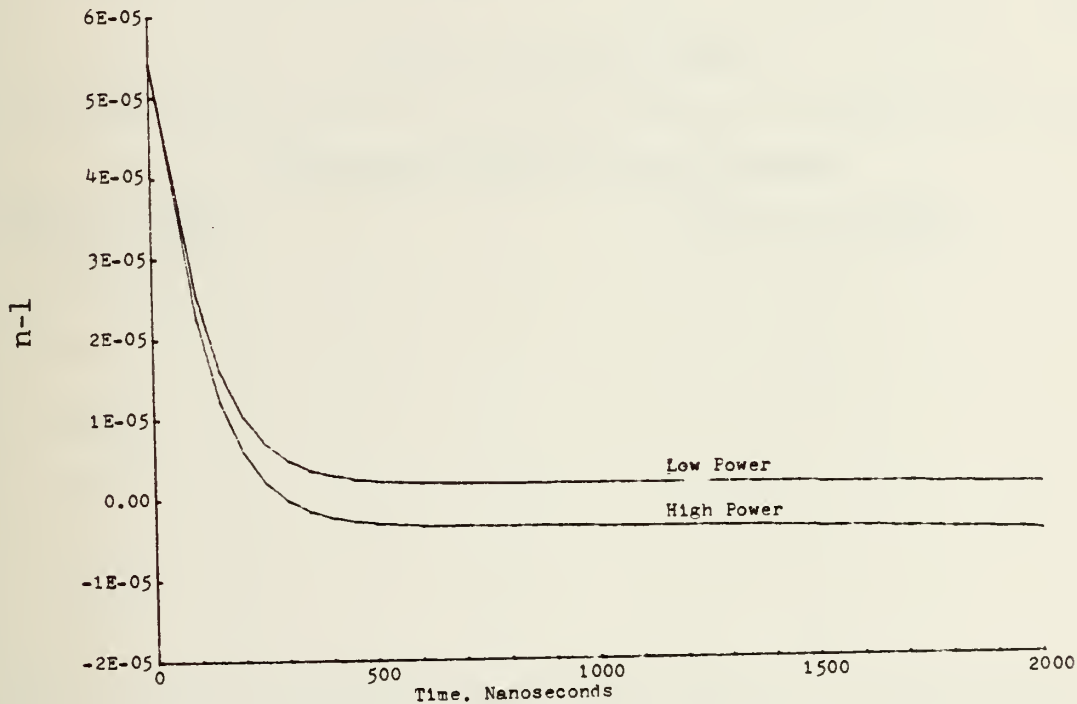
Table VIII lists the variables, symbols, and equations used in the HP9830 program to calculate n-1. Table IX lists the HP9830 program used to calculate n-1 and Tables X and XI list sample output for low and high power respectively.
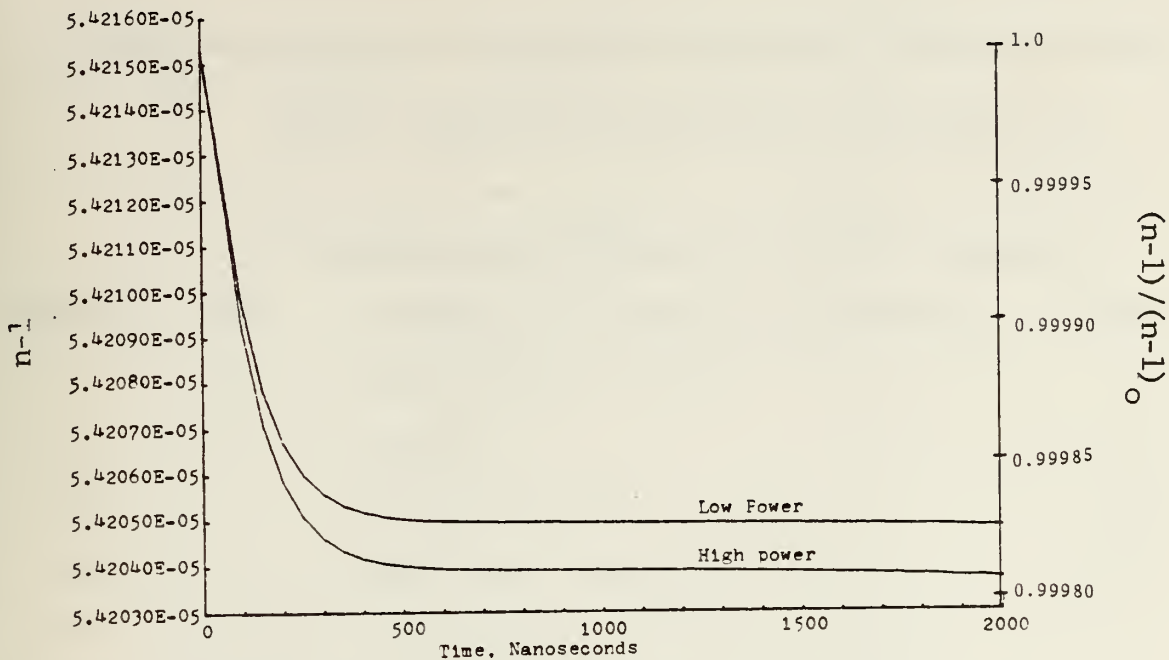
(a) Index of refraction (n-1) at laser wavelength away from 3s → 4p resonance for high and low power.

(b) Index of refraction (n-1) at laser wavelength near 3s → 4p resonance for high and low power.

Figure 9. Calculated index of refraction (n-1) as a function of time.

TABLE VIII. Variables, Symbols, and Equations Used in HP9830 Computer Program for Calculation of n-1.

Variables and Symbols Used in the Program

HP9830	Text	Meaning or Value (for constants)	Units
G	g	degeneracy (Σ 2J+1)	-
E	E	energy	cm^{-1}
C1	c	speed of light	cm/sec
K2	k	Boltzmann constant	eV/°K
M	n-1/Ne()	Contribution of excited state	-
K	2p,3s,..	Index of the levels 1 to 12	-
K()	T	Temperature	degrees Kelvin
J	-	Time increment index	-

Equations Used in the Program

Line Number	Equation Number
320	57
930	56
1030	54
1060	55
1130	53
1360	52

TABLE IX.   Listing of the HP9330 Index of Refraction (n-1)
            Program.

```
10 PRINT "            LOW POWER 10A/CM↑2"
20 PRINT
100 DATA 0,9.716E+19,1E-50,1E-50
110 DATA 50,9.716E+19,2.85E+13,1.166E+13
120 DATA 100,9.716E+19,5.314E+13,2.802E+13
130 DATA 150,9.716E+19,7.709E+13,4.034E+13
140 DATA 200,9.716E+19,8.868E+13,4.843E+13
150 DATA 250,9.716E+19,9.572E+13,5.35E+13
160 DATA 300,9.716E+19,9.998E+13,5.661E+13
170 DATA 350,9.716E+19,1.026E+14,5.851E+13
180 DATA 400,9.716E+19,1.041E+14,5.966E+13
190 DATA 450,9.716E+19,1.051E+14,6.035E+13
200 DATA 500,9.716E+19,1.057E+14,6.077E+13
210 DATA 550,9.716E+19,1.06E+14,6.103E+13
220 DATA 600,9.716E+19,1.062E+14,6.118E+13
230 DATA 650,9.716E+19,1.063E+14,6.127E+13
240 DATA 700,9.716E+19,1.064E+14,6.132E+13
250 DATA 750,9.716E+19,1.065E+14,6.135E+13
260 DATA 800,9.716E+19,1.065E+14,6.137E+13
270 DATA 850,9.716E+19,1.065E+14,6.138E+13
280 DATA 900,9.716E+19,1.066E+14,6.139E+13
290 DATA 950,9.716E+19,1.066E+14,6.14E+13
300 DATA 1000,9.716E+19,1.066E+14,6.14E+13
310 DATA 1050,9.716E+19,1.066E+14,6.14E+13
320 DATA 1100,9.716E+19,1.067E+14,6.14E+13
330 DATA 1150,9.716E+19,1.067E+14,6.141E+13
340 DATA 1200,9.716E+19,1.067E+14,6.141E+13
350 DATA 1250,9.716E+19,1.067E+14,6.141E+13
360 DATA 1300,9.716E+19,1.068E+14,6.142E+13
370 DATA 1350,9.716E+19,1.068E+14,6.142E+13
380 DATA 1400,9.716E+19,1.069E+14,6.143E+13
390 DATA 1450,9.716E+19,1.069E+14,6.144E+13
400 DATA 1500,9.716E+19,1.07E+14,6.145E+13
410 DATA 1550,9.716E+19,1.07E+14,6.146E+13
420 DATA 1600,9.716E+19,1.071E+14,6.147E+13
430 DATA 1650,9.716E+19,1.072E+14,6.148E+13
440 DATA 1700,9.716E+19,1.073E+14,6.149E+13
450 DATA 1750,9.716E+19,1.074E+14,6.15E+13
460 DATA 1800,9.716E+19,1.074E+14,6.152E+13
470 DATA 1850,9.716E+19,1.075E+14,6.153E+13
480 DATA 1900,9.716E+19,1.077E+14,6.155E+13
490 DATA 1950,9.716E+19,1.078E+14,6.157E+13
500 DATA 2000,9.716E+19,1.079E+14,6.159E+13
510 DIM T[41],K[41],S[41],Z[41],M[13],G[13]
515 DIM R[41,12],L[41],H[41],E[13],A[41,12],N[41,12]
```

```
518 Y=0
520 G[1]=1
530 G[2]=G[4]=G[7]=G[12]=12
540 G[3]=G[6]=G[10]=36
550 G[5]=G[8]=G[11]=73
560 G[9]=84
570 E[1]=0
580 E[2]=134674.61
590 E[3]=150197.81
600 E[4]=158950.1
610 E[5]=161874.4
620 E[6]=163180.29
630 E[7]=166123.23
640 E[8]=166500
650 E[9]=166562
660 E[10]=167812.5
670 E[11]=168000
680 E[12]=168750
690 K2=8.6171E-05
691 C1=2.997925E+10
692 H=4.1356E-15
693 C2=C1*H
700 C=1E-27
705 Y=Y+1
710 FOR J=1 TO 41
720 READ T[J],N[J,1],N[J,2],Z[J]
730 NEXT J
740 FOR J=1 TO 41
770 NEXT J
790 FOR J=1 TO 41
800 Q=N[J,2]*G[1]/(N[J,1]*G[2])
810 Q=LOGQ
820 K[J]=-((E[2]-E[1])*C2)/(Q*K2)
850 NEXT J
880 FOR J=1 TO 41
900 FOR K=4 TO 12
910 Q1=((E[K]-E[3])*C2)/(K2*K[J])
920 Q1=EXP(-Q1)
930 A[J,K]=G[K]*Q1/G[3]
960 NEXT K
980 NEXT J
990 FOR J=1 TO 41
1000 S=1
1020 FOR K=4 TO 12
1030 S=S+A[J,K]
1040 NEXT K
1050 S[J]=S
1060 N[J,3]=Z[J]/S[J]
1090 NEXT J
```

```
1100 FOR J=1 TO 41
1120 FOR K=4 TO 12
1130 N[J,K]=N[J,3]*A[J,K]
1160 NEXT K
1170 NEXT J
1210 M[1]=558
1220 M[2]=-87444
1230 M[3]=-59674
1240 M[4]=-58722
1250 M[5]=31324
1260 M[6]=-61758
1270 M[7]=-54918
1280 M[8]=27817
1290 M[9]=0
1300 M[10]=-32435
1310 M[11]=48799
1320 M[12]=84238
1330 FOR J=1 TO 41
1340 R=0
1350 FOR K=1 TO 12
1360 R[J,K]=M[K]*N[J,K]+C
1370 R=R+R[J,K]
1400 NEXT K
1412 IF Y=1 THEN 1418
1414 H[J]=R
1416 GOTO 1420
1418 L[J]=R
1420 PRINT "N - 1 IS"R"AT TIME"T[J]"NSEC"
1440 NEXT J
1450 PRINT
1460 PRINT "          HIGH POWER 11A/CM↑2   "
1465 PRINT
1468 IF Y >= 2 THEN 1500
1470 GOTO 705
1500 SCALE 0,2000,-2E-05,6E-05
1510 XAXIS -2E-05,100
1520 YAXIS 0,1E-05
1530 FOR J=1 TO 41
1540 PLOT T[J],L[J]
1550 NEXT J
1560 PEN
1570 FOR J=1 TO 41
1580 PLOT T[J],H[J]
1590 NEXT J
1600 PEN
1610 STOP
```

```
5000 PRINT "DATA FOR HIGH POWER 11A/CM†2"
5010 DATA 0,9.716E+19,1E-50,1E-50
5020 DATA 50,9.716E+19,3.136E+13,1.283E+13
5030 DATA 100,9.716E+19,6.398E+13,3.083E+13
5040 DATA 150,9.716E+19,8.486E+13,4.439E+13
5050 DATA 200,9.716E+19,9.762E+13,5.329E+13
5060 DATA 250,9.716E+19,1.054E+14,5.886E+13
5070 DATA 300,9.716E+19,1.101E+14,6.229E+13
5080 DATA 350,9.716E+19,1.129E+14,6.438E+13
5090 DATA 400,9.716E+19,1.147E+14,6.564E+13
5100 DATA 450,9.716E+19,1.157E+14,6.641E+13
5110 DATA 500,9.716E+19,1.163E+14,6.687E+13
5120 DATA 550,9.716E+19,1.167E+14,6.715E+13
5130 DATA 600,9.716E+19,1.17E+14,6.732E+13
5140 DATA 650,9.716E+19,1.171E+14,6.742E+13
5150 DATA 700,9.716E+19,1.172E+14,6.748E+13
5160 DATA 750,9.716E+19,1.173E+14,6.751E+13
5170 DATA 800,9.716E+19,1.173E+14,6.754E+13
5180 DATA 850,9.716E+19,1.173E+14,6.755E+13
5190 DATA 900,9.716E+19,1.174E+14,6.756E+13
5200 DATA 950,9.716E+19,1.174E+14,6.757E+13
5210 DATA 1000,9.716E+19,1.175E+14,6.757E+13
5220 DATA 1050,9.716E+19,1.175E+14,6.758E+13
5230 DATA 1100,9.716E+19,1.175E+14,6.758E+13
5240 DATA 1150,9.716E+19,1.176E+14,6.759E+13
5250 DATA 1200,9.716E+19,1.176E+14,6.76E+13
5260 DATA 1250,9.716E+19,1.177E+14,6.76E+13
5270 DATA 1300,9.716E+19,1.178E+14,6.671E+13
5280 DATA 1350,9.716E+19,1.178E+14,6.762E+13
5290 DATA 1400,9.716E+19,1.179E+14,6.763E+13
5300 DATA 1450,9.716E+19,1.18E+14,6.765E+13
5310 DATA 1500,9.716E+19,1.181E+14,6.766E+13
5320 DATA 1550,9.716E+19,1.182E+14,6.768E+13
5330 DATA 1600,9.716E+19,1.183E+14,6.769E+13
5340 DATA 1650,9.716E+19,1.184E+14,6.771E+13
5350 DATA 1700,9.716E+19,1.186E+14,6.773E+13
5360 DATA 1750,9.716E+19,1.187E+14,6.776E+13
5370 DATA 1800,9.716E+19,1.188E+14,6.778E+13
5380 DATA 1850,9.716E+19,1.19E+14,6.781E+13
5390 DATA 1900,9.716E+19,1.192E+14,6.784E+13
5400 DATA 1950,9.716E+19,1.192E+14,6.787E+13
5410 DATA 2000,9.716E+19,1.196E+14,6.791E+13
5420 END
```

TABLE X.   Output of the HP9830 for n-1 at Low Power.

```
                  LOW POWER 10A/CM↑2

   N - 1 IS 5.42153E-05     AT TIME 0       NSEC
   N - 1 IS 5.42126E-05     AT TIME 50      NSEC
   N - 1 IS 5.42097E-05     AT TIME 100     NSEC
   N - 1 IS 5.42078E-05     AT TIME 150     NSEC
   N - 1 IS 5.42067E-05     AT TIME 200     NSEC
   N - 1 IS 5.42060E-05     AT TIME 250     NSEC
   N - 1 IS 5.42056E-05     AT TIME 300     NSEC
   N - 1 IS 5.42053E-05     AT TIME 350     NSEC
   N - 1 IS 5.42052E-05     AT TIME 400     NSEC
   N - 1 IS 5.42051E-05     AT TIME 450     NSEC
   N - 1 IS 5.42050E-05     AT TIME 500     NSEC
   N - 1 IS 5.42050E-05     AT TIME 550     NSEC
   N - 1 IS 5.42050E-05     AT TIME 600     NSEC
   N - 1 IS 5.42050E-05     AT TIME 650     NSEC
   N - 1 IS 5.42050E-05     AT TIME 700     NSEC
   N - 1 IS 5.42049E-05     AT TIME 750     NSEC
   N - 1 IS 5.42049E-05     AT TIME 800     NSEC
   N - 1 IS 5.42049E-05     AT TIME 850     NSEC
   N - 1 IS 5.42049E-05     AT TIME 900     NSEC
   N - 1 IS 5.42049E-05     AT TIME 950     NSEC
   N - 1 IS 5.42049E-05     AT TIME 1000       NSEC
   N - 1 IS 5.42049E-05     AT TIME 1050       NSEC
   N - 1 IS 5.42049E-05     AT TIME 1100       NSEC
   N - 1 IS 5.42049E-05     AT TIME 1150       NSEC
   N - 1 IS 5.42049E-05     AT TIME 1200       NSEC
   N - 1 IS 5.42049E-05     AT TIME 1250       NSEC
   N - 1 IS 5.42049E-05     AT TIME 1300       NSEC
   N - 1 IS 5.42049E-05     AT TIME 1350       NSEC
   N - 1 IS 5.42049E-05     AT TIME 1400       NSEC
   N - 1 IS 5.42049E-05     AT TIME 1450       NSEC
   N - 1 IS 5.42049E-05     AT TIME 1500       NSEC
   N - 1 IS 5.42049E-05     AT TIME 1550       NSEC
   N - 1 IS 5.42049E-05     AT TIME 1600       NSEC
   N - 1 IS 5.42049E-05     AT TIME 1650       NSEC
   N - 1 IS 5.42049E-05     AT TIME 1700       NSEC
   N - 1 IS 5.42049E-05     AT TIME 1750       NSEC
   N - 1 IS 5.42049E-05     AT TIME 1800       NSEC
   N - 1 IS 5.42049E-05     AT TIME 1850       NSEC
   N - 1 IS 5.42048E-05     AT TIME 1900       NSEC
   N - 1 IS 5.42048E-05     AT TIME 1950       NSEC
   N - 1 IS 5.42048E-05     AT TIME 2000       NSEC
```

TABLE XI. Output of the HP9830 for n-1 at High Power.

```
                HIGH POWER 11A/CM↑2

    N - 1 IS 5.42153E-05     AT TIME 0      NSEC
    N - 1 IS 5.42123E-05     AT TIME 50     NSEC
    N - 1 IS 5.42091E-05     AT TIME 100    NSEC
    N - 1 IS 5.42071E-05     AT TIME 150    NSEC
    N - 1 IS 5.42058E-05     AT TIME 200    NSEC
    N - 1 IS 5.42051E-05     AT TIME 250    NSEC
    N - 1 IS 5.42046E-05     AT TIME 300    NSEC
    N - 1 IS 5.42043E-05     AT TIME 350    NSEC
    N - 1 IS 5.42042E-05     AT TIME 400    NSEC
    N - 1 IS 5.42041E-05     AT TIME 450    NSEC
    N - 1 IS 5.42040E-05     AT TIME 500    NSEC
    N - 1 IS 5.42040E-05     AT TIME 550    NSEC
    N - 1 IS 5.42039E-05     AT TIME 600    NSEC
    N - 1 IS 5.42039E-05     AT TIME 650    NSEC
    N - 1 IS 5.42039E-05     AT TIME 700    NSEC
    N - 1 IS 5.42039E-05     AT TIME 750    NSEC
    N - 1 IS 5.42039E-05     AT TIME 800    NSEC
    N - 1 IS 5.42039E-05     AT TIME 850    NSEC
    N - 1 IS 5.42039E-05     AT TIME 900    NSEC
    N - 1 IS 5.42039E-05     AT TIME 950    NSEC
    N - 1 IS 5.42039E-05     AT TIME 1000      NSEC
    N - 1 IS 5.42039E-05     AT TIME 1050      NSEC
    N - 1 IS 5.42039E-05     AT TIME 1100      NSEC
    N - 1 IS 5.42039E-05     AT TIME 1150      NSEC
    N - 1 IS 5.42039E-05     AT TIME 1200      NSEC
    N - 1 IS 5.42039E-05     AT TIME 1250      NSEC
    N - 1 IS 5.42039E-05     AT TIME 1300      NSEC
    N - 1 IS 5.42039E-05     AT TIME 1350      NSEC
    N - 1 IS 5.42039E-05     AT TIME 1400      NSEC
    N - 1 IS 5.42038E-05     AT TIME 1450      NSEC
    N - 1 IS 5.42038E-05     AT TIME 1500      NSEC
    N - 1 IS 5.42038E-05     AT TIME 1550      NSEC
    N - 1 IS 5.42038E-05     AT TIME 1600      NSEC
    N - 1 IS 5.42038E-05     AT TIME 1650      NSEC
    N - 1 IS 5.42038E-05     AT TIME 1700      NSEC
    N - 1 IS 5.42038E-05     AT TIME 1750      NSEC
    N - 1 IS 5.42038E-05     AT TIME 1800      NSEC
    N - 1 IS 5.42038E-05     AT TIME 1850      NSEC
    N - 1 IS 5.42037E-05     AT TIME 1900      NSEC
    N - 1 IS 5.42037E-05     AT TIME 1950      NSEC
    N - 1 IS 5.42037E-05     AT TIME 2000      NSEC
```

VII. CALCULATION OF PHASE SHIFT

Beam quality as previously mentioned depends on favorable illumination of the exit aperture; favorable illumination implies near constant phase. Therefore, calculation of the phase shift is important. To calculate the phase shift consider a laser cavity of length L as shown in Figure 10.
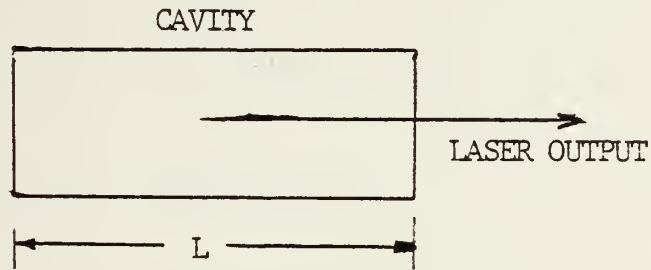

Figure 10. Geometry of Cavity

Other symbols essential for the calculation are

N - number of waves λ - wavelength

1 - denotes low power   n - index of refraction

2 - denotes high power ν - frequency of the laser

The number of waves in length L is given by

$$N_i = L/\lambda_i \qquad (59)$$

In equation (59) $i = 1, 2$. Wavelength is related to index of refraction by

$$\lambda_i = V_i / \nu = \frac{c}{n_i \nu} \tag{60}$$

Consider two regions in the cavity which are pumped at different power inputs. The difference in the number of waves in the two regions is

$$N_2 - N_1 = L \left(\frac{1}{\lambda_2} - \frac{1}{\lambda_1} \right) \tag{61}$$

Substituting equation (60) into equation (61) yields

$$N_2 - N_1 = L \left(\frac{n_2 \nu}{c} - \frac{n_1 \nu}{c} \right) = \frac{L \nu}{c} (n_2 - n_1) \tag{62}$$

Multiplying the right hand side of equation (62) above and below by n_1 produces

$$N_2 - N_1 = \frac{L \nu \, n_1}{c} \left(\frac{n_2 - n_1}{n_1} \right) \tag{63}$$

Multiplying equation (63) by $1/L$ and substituting equation (60) yields

$$\frac{N_2 - N_1}{L} = \frac{1}{\lambda_1} \left(\frac{n_2 - n_1}{n_1} \right) \tag{64}$$

The term on the left hand side is the phase shift per unit length of cavity. The phase shift at 1000 nanoseconds for a nonresonance wavelength is now calculated.

$$\lambda = 353 \text{ nm} = 353.0\text{E-7 cm (Figure 8)}$$

64

From Tables X and XI the values of n are

$n_2 = 1 + 5.42039E-05$

$n_1 = 1 + 5.42049E-05$

Substituting into equation (64)

$$\frac{N_2 - N_1}{L} = \frac{1}{353.0E-7} \left(\frac{1.0000542039 - 1.0000542049}{1.0000542049} \right) = -2.8327E-5 \text{ cm}^{-1}$$

The phase shift at 1000 nanoseconds for resonance is calculated below.

$$\lambda = 351.6E-7$$

The values of n are

$n_2 = 1 + (-3.71283E-06)$

$n_1 = 1 + (1.6602E-06)$

Substituting into equation (64)

$$\frac{N_2 - N_1}{L} = \frac{1}{351.6E-7} \left(\frac{.999996287170 - 1.000005602}{1.000005602} \right) = -8.959E-3 \text{ cm}^{-1}$$

The Strehl ratio, which is discussed by Born and Wolfe [21], provides a criterion for beam quality in terms of phase distortion. The ratio is

$$I = I_o \exp \left[-(2\pi\delta/\lambda)^2 \right] \qquad (65)$$

where I is beam intensity in the far field due to a phase distortion of δ/λ. Based on equation (65), the criterion of

$$\delta/\lambda \leq 0.1 \tag{66}$$

is frequently invoked for satisfactory beam quality. Comparing equations (65) and (61) one notes that

$$N_2 - N_1 = \delta/\lambda \tag{67}$$

The maximum length of the laser cavity, L, for good beam quality is

$$L = \frac{\delta/\lambda}{\{\frac{N_2-N_1}{L}\}} = \frac{(N_2-N_1)}{(\frac{N_2-N_1}{L})} \tag{68}$$

Substitution of numerical values yields the following results:

- maximum L for a laser operating at a nonresonant wavelength is 35 meters.
- maximum L for a laser operating at a resonant wavelength is 0.1116 meters.

For a nonresonant laser wavelength, a laser cavity with length, L, less than 35 meters will have δ/λ less than 0.1. However, if the laser wavelength is in resonance with neon, a length of laser cavity of only 0.1116 meters will cause $\delta/\lambda = 0.1$. Recall the power into the laser cavity was varied by 10 percent.

VIII. RESULTS

For a power variation of 10 percent the phase shift at nonresonance is small ($N_2 - N_1 = -0.0028$ for a 100 cm cavity) and is dominated by the neon ground state whose population is approximately one million times larger than the other species. However, in the resonance case, if the assumed values of R^* are correct, the index of refraction can be greatly magnified, resulting in a phase shift of $-8.959E-3$ cm^{-1} as compared to $-2.8327E-5$ cm^{-1} for nonresonance.

It should be noted that the populations of the neon excited states were calculated using an arbitrary choice to determine the rate constants. However, the population of Ne is approximately six orders of magnitude larger than the neon excited states and thus dominates. As long as the laser is operated away from the $3s \rightarrow 4p$ resonant wavelengths, the phase shift will be negligibly small resulting in satisfactory beam quality.

APPENDIX A

KINETIC REACTIONS AND RATE CONSTANTS FOR XeF SIMULATION

No.						Rate	
1)	(NX47)	NF	EBEM	---->	NF+	E-	EBEM	4.20CE-18	EBEM LP98
2)	(NE10)	NF	EBEM	---->	NF*1	E-	EBEM	9.25CE-19	FBEM
3)	(NX20)	NF	EBEM	---->	NF*2	E-	EBEM	2.75CE-19	FBEM
4)	(FDC5)	F2	E-	---->	F-	F	5.000E-09	ATCH PC38
5)	(FD32)	NF3	E-	---->	F-	NF2	5.000E-09	ATCH PC38
6)	(FD45)	NF2	E-	---->	F-	NF	1.000E-09	ATCH CAC6
7)	(FD40)	NF	E-	---->	F-	N	1.000E-09	ATCH G2C8
8)	(FD10)	F*	E-	---->	F	E-	5.000E-09	SUPR TF28
9)	(NE10)	NF*1	E-	---->	NF	E-	1.600E-10	SUPR
10)	(NE20)	NF*2	E-	---->	NF	E-	4.000E-11	SUPP
11)	(XE12)	XE*	E-	---->	XE	E-	2.000E-09	SUPS
12)	(NE11)	NF2+	E-	---->	NF	NF	3.150E-08	RCMP
13)	(NE21)	NF2+	E-	---->	NF2	NF	3.500E-09	RCMP
14)	(NF11)	NF3+	E-	---->	NF*1	NF	2.650E-08	RCMP
15)	(NE21)	NF3+	E-	---->	NF2	NF	1.500E-09	RCMP
16)	(XE41)	XE2+	E-	---->	XE*	XE	3.000E-07	RCMP SB27
17)	(XE39)	XE2+	E-	---->	XE*	XE	3.000E-07	RCMB GA35
18)	(NX20)	XEAF+	E-	---->	XE*	NF	6.000E-08	PCMP GA97
19)	(NX11)	XE2+	E-	---->	XE*	XE	3.600E-08	RCMP
20)	(NX21)	XENF+	E-	---->	NF*2	XF	2.400E-08	RCMP
21)	(FE11)	NF*1	NL	---->	NF2*	NE	NE	4.000E-34
22)	(FE21)	NE*2	NF	---->	NF2*	NE	NE	1.000E-34
23)	(NF22)	NF*1	NF	---->	NF*	NF	NFCH9F	1.000E-02 L	5R95
24)	(NE20)	NF+	NF	---->	NF2+	NF	NF	4.600E-32	COC3
25)	(NE54)	NF2+	NF	---->	NF3+	NF	NF	4.600E-32	3C91

```
< 26> (NE35) NE3+   NE              ----> NE2+   NE     NE                 2.000E-12         GUES
< 27> (XE19) XE*    XE     NE       ----> XE2*   NE                        1.600E-32         SR58
< 28> (XE21) XE*    XE     XE       ----> XE2*   XE                        5.000E-32         CR97
< 29> (XE28) XE2*                   ----> XE     XE     HNU3               3.330E 01 L       SP93
< 30> (XE33) XE+    XE     NE       ----> XE2+   NE                        1.000E-31         AP67
< 31> (XE34) XE+    XE     XE       ----> XE2+   XE                        2.000E-31         AP67
< 32> (XE38) XE2+   XE     NE       ----> XE3+   NE                        6.000E-32         GA97
< 33> (XE40) XE3+   XE              ----> XE2+   XE     XE                 1.700E-13         AP77
< 34> (NX12) NE*1   XE              ----> XE+    E-     NE                 4.440E-11   PENG
< 35> (NX22) NE*2   XE              ----> XE+    E-     NE                 2.960E-11   PENG
< 36> (NX13) NE*1   XE              ----> NEXE+  E-                        1.320E-11   PENG
< 37> (NX22) NE*2   XE              ----> NEXE+  E-                        8.800E-12   PENG
< 38> (NX12) NE2*   XE              ----> XE+    E-     NE     NE          7.500E-11   PENG  SR58
< 39> (NX13) NE2*   XE              ----> NEXE+  E-     NE                 2.300E-11   PENG  GA28
< 40> (NX34) NE+    XE              ----> XE+    NE                        1.000E-14 U       JM38
< 41> (NX17) NE+    NE     XE       ----> XENE+  NE                        1.000E-32         AP77
< 42> (NX16) NE2+   XE              ----> XE+    NE     NE                 5.000E-14 U       JM38
< 43> (NX19) NE2+   XE              ----> NEXE+  NE                        5.000E-14 U       JM38
< 44> (NX21) NEXE+  NE              ----> XE+    NE     NE                 3.000E-12         GUB7
< 45> (NX36) NEXE+  XE              ----> XE2+   NE                        2.000E-10         AP77
< 46> (NX37) NEXE+  XE              ----> XE+    XE     NE                 2.000E-11         TEA8
< 47> (NX23) NE3+   XE              ----> XE+    NE     NE     NE          5.000E-14         GU97
< 48> (NX28) XE+    NE     NE       ----> NEXE+  NE                        1.000E-31         AP67
< 49> (NX29) XENE+                  ----> NEXE+                            1.000E 01 L       GL97
< 50> (NX31) XENE+  NE              ----> NE2+   XE                        5.000E-14         GU97
```

<126>	(XV35)	XEF+C	NE		XEF+V	NF	NF	FORMC		GACE	3.03CF-35
<127>	(XV31)	XEF+V	NL		XEF+V	NL	QUFN	QUEN		GACB	7.4CCF-13
<128>	(XV39)	XEF+V	NL	AL	XEF+C	NE	NE	NE	QUEN	GACB	1.34CF-33
<129>	(XV40)	XEF+V	NE	NE	XEF+V	NE	NE	QUEN		GACB	1.24CF-33
<130>	(XV17)	XEF+V	F2		XEF+V	F2	F2	QUEN		GACB	3.8CCF-1C
<131>	(XV35)	XEF+V	XE		XE	XF	XF	QUEN		GICB	C.0CCF-11
<132>	(XV32)	XEF+V	AF		XEF+C	XE	QUEN	QUEN		CAC9	4.7CCF-11
<133>	(XV34)	XEF+V	NE		XF	F	NE	NE		CAC8	7.7CCF-13
<134>	(XV04)	XEF+V	NE		XE	F	NE340F	QUEN		GACB	1.42CF-01 L
<135>	(XV02)	XEF+V	NE		XEF+V	NE	NE			CUCB	1.CCCF-11
<136>	(XV03)	XEF+	NE		XEF+V	NE	NE			CUCB	1.0CCF-11
<137>	(XF4X)	F2	XE		XEF+V	F	FORMI	FORMC		CHG*	6.5CCF-11
<138>	(XF13)	XL+	F2		XEF+C	F	FORMN			CHG*	3.7CCF-10
<139>	(XF14)	XEX	NF2		XEF+V	NF	FORMN			CHG*	9.CCCF-11
<140>	(XF15)	XEX	NF5		XEF+V	NF	FORMN			VFHC	9.0CCF-11
<141>	(XF25)	XEX	NE		XEF+C	NF	FORMN			CACB	1.0CCF-10
<142>	(XF21)	XE2+	F2		XEF+C	F	F	FORMN		CAA7	7.5CCF-10
<143>	(XF22)	XF2X	NF5		XEF+V	NF2	NF2	FORMN		SR5B	2.5CCF-11
<144>	(XF23)	XE+	F-	FORMI	XEF+C	F				CHC*	1.5CC-06
<145>	(XF26)	XE2+	F-		XEF+V	XE	FORMI	FORMI		CHG*	1.5CCF-06
<146>	(XF27)	XEX5+	F-		XEF+V	NE	FORMI	FORMI		CHC*	1.5CCF-06
<147>	(XF28)	XE3+	F-		XEF+V	XE	XE	FORMI		CACB	3.0CCF-05
<148>	(XF29)	XEF+C	NE		XEF+C	NE	FORMC			CHC*	1.7CCF-14
<149>	(XF30)	XEF+C	XE		XEF+V	XE	FORMC			CS7B	2.13CF-12
<150>	(XF31)	XEF+C	NF5		XEF+C	NF3	FORMC			RJ53	2.44CF-12

<1/6> (A109) HN3S2L
<177> (AA02) XE+   NE
<176> (AA03) XE   F   NE
<179> (AA02) F-   HN352L
<160> (AA03) FZ   HN352L
<161> (AA04) XE2+   HN352L
<162> (AA09) NE2+   HN352L
<163> (AA17) NE2+   HN352L
<164> (AA21) NE2+   HN352L
<165> (AA15) XE2+   HN352L

-----> HN3S2O
-----> XE   +   NE
-----> XE   NE
-----> F   F-
-----> F   F
-----> XE+   XE
-----> NE+   NE
-----> NE1   NE
-----> NE+Z   NE
-----> XE+   XE

0.0   M   EACT   TF97
5.6CCE-12   CACT   TF97
1.CCCE-3C   P   LPCB
2.5CCF-18 P   AHSL   AP71
6.CCCF-21 P   AHSL   TF97
2.4CCF-17 P   AHSL   CFG*
9.6CCF-19 P   AHSL   WKR7
5.CCCF-19 P   AHSL
1.CCCF-19 P   AHSL
5.CCCE-18 P   AHSL   GUSE

75

APPENDIX B

CALCULATION OF RATE CONSTANT k_5

Consider a thin layer of active optical medium, with gain α, cm^{-1}, in the laser cavity of length ℓ, cm. The change in intensity I, watts/cm^2, within the thin layer is

$$\Delta I = I_{out} - I_{in} = \alpha I \ell \tag{69}$$

The number of photons per unit time entering the layer of active optical medium is

$$\dot{N}_{in} = \frac{I_{in} A}{h\nu} \tag{70}$$

A corresponding term for the number of photons leaving per unit time is

$$\dot{N}_{out} = \frac{I_{out} A}{h\nu} \tag{71}$$

The rate of production of photons within the thin layer is the difference between $\dot{N}_{out}$ and $\dot{N}_{in}$ which is

$$\left\{ \begin{array}{l} \text{rate of pro-} \\ \text{duction} \\ \text{of photons} \end{array} \right\} = \dot{N}_{out} - \dot{N}_{in} = \frac{A}{h\nu} (I_{out} - I_{in}) \tag{72}$$

Equation (72) neglects spontaneous emission. Combining equations (69) and (72) yields

$$\text{production rate} = \frac{\alpha A \ell I}{h\nu} \tag{73}$$

From equation (19) the rate of production of photons by stimulated emission is

$$\text{production rate} = k_5 [h\nu][KrF^*]A\ell \tag{74}$$

where the symbol $[h\nu]$ means number of photons per unit volume. The gain coefficient also is equal to

$$\alpha = \sigma[KrF^*] \tag{75}$$

where σ is the optical cross section for stimulated emission at the frequency ν. The number density of photons $[h\nu]$ is related to intensity by

$$[h\nu] = \frac{I}{ch\nu} \tag{76}$$

where c is the velocity of the photons; c, obviously, is the speed of an electromagnetic wave.

Combining equations (73) to (76) gives

$$k_5 = c\sigma \tag{77}$$

The dimensions of k_5 are cm^3/sec; the dimension of σ is cm, and c is cm^2/sec. From reference [2] the value of σ is $5.0E-16$ cm^2, and c is $3.0E10$ cm/sec. Substituting these values into equation (77) yields

$$k_5 = 1.5\text{E-}05 \ cm^3/sec$$

This is the value for k_5 used in the computer program.

APPENDIX C

CALCULATION OF PHOTON CONCENTRATION

The concentration of photons is given by equation (76)
as

$$[h\nu] = I/ch\nu$$

Assuming,

$$I = 10 \text{ k}\omega/\text{cm}^2 \text{ (saturation value)}$$
$$c = 3.0E10 \text{ cm/sec}$$
$$h = 6.6256E\text{-}34 \text{ J-sec}$$
$$\lambda_o = 248.0E\text{-}9 \text{ m}$$

the concentration of photons can be calculated.

$$[h\nu] = \frac{10.0E3}{(3.0E10)(6.6256E\text{-}34)(\frac{3.0E8}{248.0E9})}$$

$$[h\nu] = 4.159E11/\text{cm}^3 \ .$$

LIST OF REFERENCES

1. Ewing, J. J. and Brau, C. A., "High Efficiency UV Lasers," _Tunable Lasers and Applications_, Springer, Berlin, 1976.

2. Ewing, J. J., "Rare-gas Halide Lasers," _Physics Today_, Vol. 31, pp 32-39, May 1978.

3. Slater, J. M., _et al._, "UV Sustained Discharges for Rare Gas Halide Lasers," _Mathematical Sciences North-west, Inc._ MSNW 78-1074-1, 13 March 1978, Ballistic Missile Defense Advance Technology Center Contract DASG 60-77-C-0059.

4. Center, R. E., and Fisher, C. H., "Kinetics Studies for XeF and KrF Lasers," _Mathematical Sciences North-west, Inc._ MSNW 78-1062, 31 January 1978, DARPA Order No. 1806.

5. Trainor, D. W., and Mani, S. A., "Optical Conversion Processes," AVCO Everett Research Laboratory, Final Report, January 1978, DARPA Order No. 1806.

6. Denes, L. J., _et al._, "Research Program on UV Initiated Rare Gas Halide Lasers," Westinghouse R & D Center, Mid Term Technical Report, DARPA Order No. PARN 79071, July 1977.

7. Parks, J. H., "Excimer Laser Research", AVCO Everett Research Laboratory, Inc., Semi-Annual Report of Period 16 March 1977 to 15 September 1977, DARPA Order No. 1806.

8. Wang, C. P., "High-Repetition-Rate Transverse-Flow XeF Laser," _Applied Physics Letters_, Vol. 32, pp 360-362, 15 March 1978.

9. McDaniel, E. W., _et al._, "Compilation of Data Relevant to Rare Gas-Rare Gas and Rare Gas-Monohalide Excimer Lasers," School of Physics, Georgia Institute of Technology, and U.S. Army Missile R & D Command, Tech. Rep. H-78-1, Vol. I, Vol. II, December 1977.

10. Nighan, William L. and Hall, Robert J., "Investigation of Plasma Processes in Electronic Transition Lasers," United Technologies Research Center, R77-922617-2, Annual Report July 1977, ONR Contract N00014-76-C-0847.

11. Wang, C. P., "Simple Fast-Discharge Device for High-
    Power Pulsed Lasers," Rev. Sci. Inst., Vol. 47, pp 92-
    95, 1976.

12. Bennett, H. E., et al., "Ultraviolet Components for
    High Energy Applications," Naval Weapons Center, NWCTP
    6015, March 1978.

13. Ferriter, N., et al., "Analysis of Efficient Impulse
    Delivery and Plate Rupture by Laser Supported Detona-
    tion Wave," ASME, 75-WA/HT-50, 1975.

14. Bleach, R. D., and Nagel, D. J., "Craters Produced by
    High Power-Density Lasers," ASME, 75-WA/HT-49, 1975.

15. Reilly, R. D., Woodroffe, J. A., and Sutton, G.,
    "Thermo-Mechanical Plate Penetration by Repetitive-
    Pulse Lasers," AIAA Paper 78-140, 1978.

16. Fuhs, A. E., "Density Inhomogeneity in a Laser Cavity
    Due to Energy Release," AIAA Journal, Vol. 11, pp. 374-
    375, March 1973.

17. Biblarz, O., and Fuhs, A. E., "Density Changes in a
    Laser Cavity Including Wall Reflections and Kinetics
    of Energy Release," AIAA Journal, Vo. 12, pp. 1083-
    1089, 1974.

18. Biblarz, O., and Fuhs, A. E., "Laser Internal Aero-
    dynamics and Beam Quality," Society of Photographic
    and Instrumentation Engineers, Proceedings of 1973
    Annual Meeting, Vol. 41, Developments in Laser Tech-
    nology II,   , pp. 59-70.

19. Nerheim and Chen, "Visible Laser Development," Jet
    Propulsion Laboratory, DARPA Order No. 2756,
    September 1976.

20. Wright, W. E., LCDR, "Charged Particle Beam Weapons:
    Should We? Could We?" Naval Institute Proceedings,
    November 1979.

21. Born, W., and Wolf, E., Principles of Optics, Pergamon
    Press, New York, 1964, Second Edition.

22. Hogge, H. D. and Crow, S. C., Flow and Acoustics in
    Pulsed Excimer Lasers, paper presented at AIAA Con-
    ference on Fluid Dynamics of High Power Lasers, II-4,
    Cambridge, MA, 2 November 1979.

23. Fuhs, A., Etchechury, J. and Cole L., _Progress Report #2, XeF Beam Quality Considerations_, submitted to Dr. J. A. Mangano, DARPA, 25 February 1979.

24. Siegler, R., _et al._, _XeF Demonstrator Program_, Rocket-dyne International, 15 February 1979.

25. Mitchell, A.C.G., and M. W. Zemansky, _Resonance Radiation and Excited Atoms_, p. 238, Cambridge, 1934.

26. Johnson, T. H., Palumbo, L. J., and Hunter, II, A. M., "Kinetics Simulation of High-Power Gas Lasers," _IEEE Journal of Quantum Electronics_, Vol. QE-15, No. 5, May 1979.

27. Huestis, D. L., _et al._, "Quenching of Ne*, F*, and F_2* in Ne/Xe/NF_3 and Ne/Xe/F_2 Mixtures," _J. Chem. Phys._, Vol. 69, 1 December 1978.

28. McDaniel, E. W., _et al._, "Compilation of Data Relevant to Nuclear Pumped Lasers," School of Physics, Georgia Institute of Technology, and U.S. Army Missile R & D Command, Tech. Rep. H-78-1, Volume IV, December 1978.

29. Rokni, M., Jacob, J. H., and Mangano, J. A., "Dominant formation and quenching processes in E-beam pumped ArF* and KrF* Lasers," _Physical Review A_, Vol. 16, December 1977.

30. Schneider, B. I., and Brau, C. A., "Dissociative attachment of electrons to F_2," _Appl. Phys. Lett._, Vol. 33, 1 October 1978.

31. Finn, T. G., Palumbo, L. J., and Champagne, L. F., "A Kinetics Scheme for the XeF Laser," _Appl Phys. Lett._, Vol. 33, 15 July 1978.

32. Pressley, R. J., _Handbook of Lasers_, Chemical Rubber Co., Cleveland, Ohio, 1971.

33. Fuhs, A., Etchechury, J., and Cole, L., _Summary of Progress During FY 1979, Beam Quality in Excimer Lasers_, prepared for Major R. Benedict, DARPA, 15 October 1979.

34. Etchechury, J., _A Simple Model for Calculating the Index of Refraction of Neon I and Neon* (3s) in the Cavity of a Xenon Fluoride Laser_, MS in Physics Thesis, Naval Postgraduate School, Monterey, California, 1978.

35. Fuhs, A., Cole, L., and Blaisdell, G., _Progress Report No. 5, Beam Quality in Excimer Lasers_, prepared for Major R. Benedict, DARPA, August 1979.

36. Fuhs, A., Etchechury, J., and Cole, L., _Progress Report No. 3, Beam Quality in Excimer Lasers_, prepared for Dr. Joseph Mangano, DARPA, May 1979.

INITIAL DISTRIBUTION LIST

10. Dr. Robert Behringer   1
    Office of Naval Research
    Pasadena Branch Office
    1030 East Green Street
    Pasadena, California 91101

11. CAPT. Alfred Skolnick   1
    Naval Sea Systems Command
    PMS 405
    Crystal City
    Washington, D.C. 22202

12. CAPT. D. H. Johnston, Jr.   1
    Supervisor of Shipbuilding,
         Conversion, and Repair, USN
    Drawer T, Mayport Naval Station
    Jacksonville, Florida 32228

13. Lt., Lonnie W. Cole   2
    120 South Harrison Street
    East Orange, New Jersey 07018

14. Dr. Louis J. Palumbo   1
    Code 5540
    Naval Research Laboratory
    Washington, D.C. 20375

15. CAPT. James Etchechury, U.S. Army   1
    Pershing II Missile Office
    Army Missile R and D Command
    Redstone Arsenal
    Huntsville, Alabama 35807